T-AM-SymII-1 MATCHING MOLECULES: THE TROPOMYOSIN/TROPONIN SWITCH. Carolyn Cohen, Rosenstiel Basic
Medical Sciences Research Center, Brandeis University, Waltham, MA 02254.

Fibrous proteins display in extravagant ways basic features of design common to many biological molecules. They depend for their functions on precise, specific interactions, both with themselves and with other proteins. These functions may require, as well, extensive molecular motions involving substantial conformational changes. This is nowhere better illustrated than in the case of the tropomyosin/troponin switch that regulates contraction in many muscles. The role of tropomyosin in this system depends on its specific interactions both with actin and the troponin complex as well as with itself. Crystallographic and amino acid sequence analysis of this α-helical coiled-coil protein reveal a remarkable correspondence between the geometry of the tropomyosin molecule and the chemical interactions it displays. Troponin consists of three subunits, each with a different architecture and function; one of these (TnT) has unusual extended structure and binds to two widely separated sites on tropomyosin. As in many other systems, Ca^{2+} is the trigger for this switch which requires for its action both fixed and variable linkages among these many interacting proteins. Our structural results now show in some detail how this intricate fibrous protein assembly is constructed and how it may operate to control contraction.

T-AM-SymII-2   MYOSIN AMINO ACID SEQUENCE AND THE ASSEMBLY OF MUSCLE A.D. McLachlan.
MRC Laboratory of Molecular Biology, Hills Road, Cambridge, England, CB2 2QH.
The structure and the assembly of myosin filaments in muscle depend strongly on the interactions between myosin molecules, which involve both the globular S-1 head and the rodlike helical tail. The structural evidence for head-head and head-tail interactions is reviewed, and it suggests that phosphorylation is an important controlling factor. The electrostatic interactions between myosin tails which are important in building up the thick-filament arrays depend on 7-residue and 28-residue repeat patterns in the helical sequence. These seem to determine the 143A and 430A parallel staggers in the outer part of the filament. The antiparallel staggers in the bare zone will be analysed in terms of the sequences of various rod species, including nematode, rat and Acanthamoeba myosin II. A proper 3-dimensional understanding of the filaments requires a knowledge of the coiled-coil pitch. The existing evidence on the pitch will be described, and its implications for the coiled-coil packing discussed. Irregularities (skip residues) in the coiled coil at approximately 196-residue intervals may play an important part in the packing and define a longer structural unit. The N-terminal S-2 part of the myosin rod is less firmly attached to the filament surface and contains the postulated 'hinge region'. We contrast two models of the S-2, the traditional 'rigid lever arm' and the newer 'bent fishing rod', in which S-2 can peel off continuously from the surface and has elastic behaviour. Here the charges along the length of the helix provide an electrostatic surface energy of adhesion which can take up part of the mechanical strain in the muscle.

T-AM-SymII-3 STRUCTURAL CONSEQUENCES OF COLLAGEN GENETIC TYPES, Barbara Brodsky and Eric F.
Eikenberry, UMDNJ-Robert Wood Johnson Medical School, Piscataway, NJ 08854.

The molecules of five distinct genetic types of collagen (types I, II, III, V and XI) contain triple-helical domains 300 nm in length which can form fibrils with a 67 nm axial stagger and there is a specific tissue distribution of these collagen types. Comparison of their molecular and fibrillar structures may clarify the way in which different collagen molecules, through interactions with each other and with non-collagenous components, can confer required mechanical properties on various connective tissues. Type I collagen is packed in a 3-dimensional crystalline array in fibrils of tail tendons and the structure of its unit cell has recently been elucidated to a resolution of approximately 1 nm. Crystalline type II fibrils differ from those of type I in having a 40% larger unit cell, with the expansion almost entirely along one axis. Skin fibrils, which contain 85% type I and 15% type III collagen, are less ordered than type I tail tendon fibrils and have an increased shearing that results in a larger molecular tilt and decreased axial stagger. Types V and XI collagens, always found together with larger amounts of types I or II respectively, can form fibrils with a 67 nm period in vitro and therefore may be part of the major collagen fibrils in vivo.

The triple-helical regions of these fibril-forming collagens maintain glycine as every third residue and show similar spectroscopic properties. High angle x-ray diffraction studies indicate that the molecular structures of different genetic types differ in their helical parameters. Collagens which do not form characteristic staggered fibrils have been found and we have begun to examine the x-ray patterns of these molecules to determine whether collagens which are not required to pack into periodic fibrils differ in their triple-helical structures.

T-AM-SymII-4 COMPARISON OF IN VIVO AND IN VITRO MYOSIN ASSEMBLIES: ORGANIZATION INTERACTIONS AND STABILITY

Jane F. Koretz, Santa J. Tumminia, and Joseph V. Landau. Biophysics and Biochemistry Group and Department of Biology, Science Center, Rensselaer Polytechnic Institute, Troy, NY 12180-3590

Native thick filaments (NTFs) from vertebrate skeletal muscle differ structurally and morphologically from synthetic thick filaments (STFs) prepared from solutions of skeletal myosin. These differences arise at the molecular level though fundamentally distinct intermolecular interactions. The myosin molecules in STFs on either side of the bare zone are organized in identical microenvironments, while the myosin in NTFs reside in a variety of configurations dependent on longitudinal and, in the case of rabbit NTFs, radial location. The variety of configurations depends in part on the asymmetric distribution of other thick filament proteins within the NTF, but in vitro readdition of such proteins to purified myosin results in filaments that again exhibit symmetric protein distributions and interactions. These organizational differences between STFs and NTFs are further demonstrated by signficant differences in filament stability under increased hydrostatic pressure: rabbit STFs shorten linearly with increasing pressure, while rabbit NTFs break in half at the bare zone. The behavior of human and rhesus NTFs under the same experimental conditions differs both from that of the rabbit NTFs and from each other, consistent with subtle structural differences between each. Long-term glycerination of NTFs alters their behavior under increased hydrostatic pressure to a dissociation more nearly resembling that of STFs.

T-AM-SymII-5 ELASTIC CYTOSKELETAL FILAMENTS COEXIST WITH THICK AND THIN FILAMENTS WITHIN THE SARCO-
MERE. K. Wang. Clayton Foundation Biochemical Institute, Department of Chemistry and Cell Research Institute, The University of Texas at Austin, Austin, TX 78712

The sarcomere of striated muscle is widely accepted as being constructed of two sets of parallel and interdigitating protein filaments which are discontinuous and inextensible. However, recent evidence from several laboratories has indicated that there are additional filamentous constituents in the sarcomere. Biochemical, morphological and immunostaining data suggest that sarcomeres contain two sets of longitudinal, continuous and probably elastic cytoskeletal filaments as integral structural components. One set of cytoskeletal filaments coexists with thick and thin filaments within the sarcomere, and consists of the newly discovered proteins titin and nebulin; the other set is the longitudinal component of an extensive network of intermediate filaments which envelop each sarcomere and interlink other cellular organelles. Thus the cytoplasm of striated muscle cell contains a highly elaborate cytoskeletal matrix within which thick-thin filaments and other cellular organelles are integrated structurally and functionally. These lattices may have roles as structural scaffolds and may contribute to the elastic properties such as resting tension and compliance.

T-AM-A1   STRUCTURAL MODELS OF THE SODIUM CHANNEL ION SELECTIVITY, ACTIVATION, AND INACTIVATION
    H. Robert Guy (Intr. by R. Jernigan), Lab. Math. Biology, NCI, NIH, Bethesda, MD 20892

The structural model of the eel sodium channel proposed by Guy and Seetharamulu (PNAS 83:508, 1986) has been modified and extended by analyzing sequences of two rat sodium channels (Noda, et al., Nature 320:188, 1986). The channel is postulated to be formed by four homologous domains, each of which contains eight transmembrane segments, S1-S8. All putative transmembrane segments are α helices except for S7 of the last domains which is postulated to be three β strands. S6 and S7 are short and do not cross the membrane completely. The channel lining has a narrow portion formed between the four S7 segments. S7 aspartate and glutamate carboxyls can form a selectivity filter with dimensions near those proposed by Hille (J. Gen. Physiol. 58:599, 1971). All side chains of the selectivity filter are conserved between eel and rat channels. Activation is postulated to involve a "screw-like" motion of positive charges on the four S4 helices. Inactivation is postulated to involve additional movement of S4 in the last domain and blockade of the channel from the cytoplasm by a positively charged α helical hairpin located between the third and fourth homologous domains. This inactivation gate can be phosphorylated by cyclic AMP. These mechanisms can produce a kinetic scheme for channel activation and inactivation consistent with most experimental data. A principle of "unilateral conservation" is proposed in which the side of a transmembrane α helix involved in protein-protein interactions is better conserved than the side involved in protein-lipid interactions. S1, S2, and S3 have poorly conserved faces predicted to be exposed to lipid and highly conserved faces that are polar near the ends of the helices and that are postulated to interact with S6 helices in their central apolar regions.

T-AM-A2   STRUCTURE-ACTIVITY RELATIONSHIPS IN A SERIES OF SYNTHETICALLY MODIFIED BREVETOXINS ACTING ON NEURONAL SODIUM CHANNELS. G.R. Strichartz, E.A. Crill, T.A. Rando, Anesthesia Res. Labs, Brigham and Women's Hospital, Harvard Medical School, Boston, MA 02115, and T. Blizzard, G.-W. Qin, M.S. Lee, and K. Nakanishi, Dept. of Chemistry, Columbia University, New York, NY 10027.

The actions of a series of brevetoxins (BvTX) were assayed on myelinated nerve by voltage-clamp and sucrose-gap. Under voltage-clamp, BvTX-A activated a small fraction of $\overline{G_{Na}}$ at a potential 20 mV more negative than normal and also inhibited inactivation. These phenomena account for the reversible, dose-dependent depolarization (ΔV) seen under sucrose-gap; the potency order is (with EC_{50}):

BvTX-X

BvTX-F (30nM) < BvTX-D (70nM) < BvTX-E (100nM) < BvTX-B (200 nM) < BvTX-G (400nM). Maximum ΔV ($\overline{\Delta V}$) at high [BvTX] also varied with toxin, BvTX-D → 24 mV and BvTX-E → 14 mV. Although reductions of BvTX-B to the -F and -G toxins altered potency, the $\overline{\Delta V}$ of (18-19 mV) was unchanged. Pretreatment by low [veratridine] enhanced the ΔV. Pretreatment by scorpion α-toxin increased both potency and $\overline{\Delta V}$, but exposure to lidocaine before and during BvTx depressed ΔV competitively.
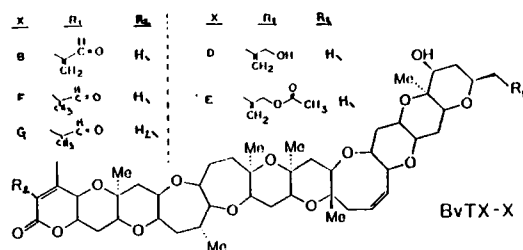
T-AM-A3   SODIUM CHANNEL SYNTHESIS IN CELL BODIES OF SQUID GIANT AXONS. Wm. F. Gilly and Tom Brismar, Hopkins Marine Station of Stanford University, Pacific Grove, CA 93950.

Giant axons in squid are formed by the fused axons from hundreds of small neurons in the giant fiber lobe (GFL) of the stellate ganglion. Somata of GFL cells normally do not show voltage dependent Na current (I_{Na}) when studied under current- or voltage-clamp. If GFL cells from Loligo opalescens are separated from their giant axons and maintained in primary culture (15°C), large I_{Na} appears in the soma membrane over 3-4 days and remains for up to 30 days thereafter. Axon regeneration does not occur under these conditions. The absolute amount of I_{Na} is proportional to cell capacitance and reaches an average maximum density of ~4 mS/cm^2 (470/110 mM Na in external/internal media). Voltage dependence and kinetics of activation and inactivation are very similar to those properties of 'ordinary' I_{Na} in giant axons of Loligo pealei studied under similar conditions. I_{Na} in GFL cells is almost eliminated by 10 nM saxitoxin at all stages of culture.

Inclusion of actinomycin D (50 g/ml) in the culture medium does not alter the initial appearance of large I_{Na} (e.g., on day 3), but then causes the amount of I_{Na} present to disappear with a time constant of ~1 day. Inclusion of the colchicine derivative demecolcine (10-50 g/ml) prevents the appearance of any I_{Na}. Incorporation of I_{Na} into the GFL cell membranes must depend on both synthesis of mRNA (and Na channel proteins) and intracellular, microtubule-associated ('axoplasmic') transport.

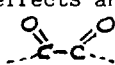**T-AM-A4** BIOSYNTHESIS AND POST-TRANSLATIONAL PROCESSING OF THE VOLTAGE-SENSITIVE SODIUM CHANNEL FROM EEL ELECTROPLAX. W.B. Thornhill and S.R. Levinson, Dept. of Physiology, Univ. of Colorado, School of Medicine, Denver, CO 80262. The eel sodium channel has been shown to be a very heavily post-translationally processed protein (M_r 260,000). Compositional analysis of the channel has shown it is 30% carbohydrate by weight and has 8% fatty acyl moieties associated with it even after SDS-gel filtration and extensive dialysis. The unusual behavior the channel exhibits on SDS-PAGE is due to these non-protein domains.

   We have used both the eel electroplax and the frog oocyte, following the injection of electroplax mRNA, to investigate the biosynthesis and post-translational processing of the sodium channel. Pulse-chase experiments with radioactive precusors to the channel followed, by immunoprecipitation of the molecule with specific antisera, indicate that the channel acquires some of its characteristic hydrophobic domains before it is completely glycosylated. Lectin binding studies of intermediately processed channels also suggest that the molecule is heavily processed in the Golgi apparatus. A number of antibiotics that specifically block post-translational modification of some membrane proteins, and their cell surface expression, have been used to help ascertain which processing events are required for the intracellular transport of the sodium channel to the cell surface.

T-AM-A5 SLOWLY INACTIVATING SODIUM CURRENTS FROM INJECTION OF HIGH MOLECULAR WEIGHT RAT BRAIN RNA INTO XENOPUS OOCYTES. D. Krafte, J. Leonard, T. Snutch, N. Davidson and H. A. Lester Divs. of Biology and Chemistry, Caltech, Pasadena, CA 91125.

   We have fractionated rat brain poly(A+) RNA on a sucrose gradient and injected the high molecular weight (MW) fraction into Xenopus oocytes. The properties of Na channels induced by this fraction, shown to contain the mRNA encoding the α subunit, have been compared with those produced by injecting unfractionated poly(A+) RNA. Na currents were measured with a standard two micro-electrode voltage clamp or a patch clamp utilizing pipettes with 25 μ meter openings. This latter method eliminates the voltage control problems one has when clamping the entire oocyte capacitance. Na currents were isolated from contaminating currents with the two microelectrode technique by sub-tracting currents before and after the addition of 500 nM TTX. With the patch clamp method contaminating currents were eliminated by soaking the oocytes in Cs+ and/or addition of 5 mM 4-AP to the bath. We found Na channels resulting from injections of high MW RNA were similar in many respects to those produced by unfractionated RNA. Both were blocked by TTX with a Kd near 5 nM and both were sensitive to scorpion toxin. Currents activated near -40 mV and peaked between -10 and 0 mV in both cases. Despite these similarities we found that the inactivation rates of sodium currents from high MW RNA alone were consistently slower than those from unfractionated RNA. Tau at -10 mV was 1.6 $\mp$ 0.1 ms for unfractionated and 3.8 $\mp$ 0.3 ms for high MW RNA. This difference was observed at test potentials more positive and more negative than -10 mV as well. The difference in kinetics possibly arises from a) the absence of RNA encoding for the small subunits of the $\alpha\beta_1\beta_2$ channel or b) the absence of RNA encoding proteins involved in post translational processing of the channel complex. Supported by NS-11756 and AHA-GLAA.

T-AM-A6 DIFFERENTIAL EFFECTS ON NA AND K CHANNEL GATING KINETICS BY AN ARGININE MODIFIER. J.F. Fohlmeister and W.J. Adelman, Jr., Lab. of Biophysics, NINCDS, NIH, Marine Biological Laboratory, Woods Hole, MA 02543 and Lab. of Neurophysiology, University of Minnesota, Minneapolis, MN 55455.

   Ionic currents obtained under square-wave voltage-clamp of squid axons internally perfused with camphorquinone-10-sulfonic acid (CSA) showed a reduced peak Na-current (with no apparent change in time constants), and a marked slowing of K-channel kinetics. 5 mM internal CSA reduces the Na-current peaks by ~ 50% and slows K-kinetics by a factor of ~ 2; 10 mM internal CSA virtually elimi-nates Na-current and slows K-kinetics by a factor of ~ 4. All effects are reversible on a time scale of minutes. CSA contains an active site with structure   that is held rigid by the remaining molecular structure; the active site   is arginine specific in proteins, and masks the positive charge of that amino acid. Assuming the in situ function is arginine modification, one may conclude that arginines are principal components of the electric field sensors in both the Na and K channels, but that the gating mechanisms of the two channels are significantly different. The slowing in K-channel kinetics is consistent with a voltage-sensor of reduced charge, as opposed to a Cole-Moore shift or related effect which might be induced by a substantial change in membrane surface charge. The ultimate elimination of Na-current in 10 mM CSA, with no apparent slowing of the kinetics at lower concentrations, suggests the possi-ble elimination of a fast channel-opening kinetic step, with little effect on slower gating kinetic transitions.

T-AM-A7   EFFECT OF CAMPHORQUINONE-10-SULFONIC ACID ON GATING CURRENT. W.J.Adelman, Jr. and J.F. Fohlmeister, Laboratory of Biophysics, NINCDS, NIH, Marine Biological Laboratory, Woods Hole, MA 02543, and Laboratory of Neurophysiology, University of Minnesota, Minneapolis, MN 55455.

Gating current obtained in dynamic steady states under sinusoidal voltage-clamp suggests the operation of two Kinetic processes (primary and secondary) in activation gating of Na-channels. Camphorquinone-10-sulfonic acid (CSA), a known reversible arginine modifier, appears to affect these kinetics in a differential fashion. 5 mM internal CSA appears to reversibly reduce the charge movement associated with the secondary kinetics, with little change in the primary kinetics. The relatively very fast secondary transitions are slowed, and the total secondary kinetic charge-movement is reduced, both by about 50 %. 10 mM internal CSA appears to reduce the charge-movement associated with the primary kinetics, and to eliminate the secondary kinetic transitions entirely. These effects are consistent with the observed effects of internal CSA on the Na-ionic currents observed under square-wave voltage-clamp, with the assumption that the secondary transitions constitute channel-opening. Attempts to interpret the CSA gating current data within the context of other existing gating kinetic models will also be discussed.

T-AM-A8   **INCORPORATION OF SODIUM CHANNELS FROM SQUID OPTIC NERVE INTO PLANAR LIPID BILAYERS.**
R. Latorre, A. Oberhauser, M. Condrescu, R. DiPolo and F. Bezanilla. *Centro de Estudios Científicos de Santiago, P.O. Box 16443, Santiago 9, Chile; Instituto Venezolano de Investigaciones Científicas, Caracas, Venezuela and Department of Physiology, UCLA, Los Angeles CA 90024.*

We have incorporated sodium channels from the squid optic nerve into planar bilayers made of pure neutral lipids. Channels were incorporated by adding a membrane fraction enriched in axolemma obtained from optic nerves of the squid *Sepiotheutis sepioidea* to one side of the bilayers. The channels were maintained open by the use of batrachotoxin (BTX) added to the aqueous solution. The channel exhibits a conductance of 18-20 pS in symmetrical 200 mM NaCl at 22° C and behaves as a sodium electrode. Under bi-ionic conditions the P_{Na}/P_K is about 10. Tetrodotoxin blocks the channel in a voltage dependent manner with an apparent dissociation constant at zero voltage of about 2 nM. We have also been able to determine the characteristics of the voltage dependence of the BTX-modified channel. The voltage at which channels are open 50% of the time was determined to be in the range of -90 to -100 mV and the apparent gating charge was four electronic charges. We found that using the ionic conditions of artificial sea water (ASW), which contains 50 mM $MgCl_2$ and 10 mM $CaCl_2$, the channel conductance is reduced to about 2 pS at negative potentials. Furthermore, under these conditions, the probability of opening is shifted to more depolarizing potentials. We conclude that the sodium channel from the squid optic nerve has similar characteristics to those shown by BTX-modified sodium channels from mammalian muscle and brain incorporated in bilayers. We suggest that the differences between BTX-modified sodium channels recorded from *in vivo* squid preparation and those obtained in bilayers are only due to the high divalent concentration of ASW. *We thank Dr. J. Daly for providing BTX. Supported by NIH grants GM35981, GM30376 and the Tinker Foundation.*

T-AM-A9   **SINGLE SODIUM CHANNELS RECORDED FROM THE CUT-OPEN SQUID GIANT AXON.** F. Bezanilla. *Department of Physiology, UCLA, Los Angeles, CA 90024.*

The modified cut-open axon technique was used to record single channel events from the internal surface of the squid giant axon. The axon was cut open in artificial sea water (ASW = 440 mM Na, 10 mM Ca, 50 mM Mg, 10 tris). The solution was then exchanged to 540 mM Na and 10 mM tris with no added Ca or Mg. Patch pipettes with tip diameters less than 1 um filled with 45 mM Na and N-methylglucamine as a cationic replacement, were approached to the internal surface of the axon with 320X magnification and gigaohm seals were obtained. To decrease the number of active sodium channels under the patch, the internal membrane surface was exposed to ASW for a few minutes before the seal was attempted. Under these conditions, up to two sodium channels could be recorded in the patch and they could be resolved in the range of -50 to -20 mV. The single channel conductance ranges between 12 and 15 pS at 4 to 6 °C. This result is comparable to the single channel conductance recorded from the optic nerve sodium channel incorporated in bilayers (Latorre et al. ,Biophys. J., 1987, these proceedings) in conditions of zero divalent cations and scaled with a Q_{10} of 1.3 to correct for the temperature difference. Events show openings with fast interruptions giving a mean open time of 0.4 to 0.6 ms at -40 mV. These results show that single sodium channels can be recorded from the squid axon in conditions of zero external divalent cations, that patches survive in zero divalent conditions and that the single channel conductance of the sodium channel in squid is not too different to the values recorded in other preparations. The value reported here is much larger than the single channel conductance previously reported as estimated by noise analysis. The most likely explanation is that under normal conditions channels are partially blocked by the high concentration of Ca and Mg normally present in the ASW. Supported by NIH grant GM 30376.

T-AM-A10   STRUCTURE-FUNCTION RELATIONSHIPS OF THE SODIUM CHANNEL STUDIED BY SPECIFIC ANTIBODIES AND SYNTHETIC PEPTIDE FRACTIONS OF THE CHANNEL MOLECULE
H. Meiri, G. Spira, M. Sammar, Y. Rosenthal, Y. Palti and A. Komoriya*. Rappaport Institute and Faculty of Medicine, Technion, Haifa, Israel, and *BRC Meloy, Rockville, MD, USA.

Sodium channels were studied by voltage clamping single myelinated nerve fibers from frog and patch clamping rat DRG cells grown in tissue culture. Monoclonal antibody SC-72-38, generated against the sodium channels of the eel electroplax membrane, was used as a primary probe. The mAb was found to specifically modify the sodium channel conductance inactivation and activation. The voltage dependency of the steady-state inactivation as well as the steady-state activation of the channel were significantly shifted towards more negative potential values. The voltage dependency of the channel inactivation kinetics (τ_h) was also modified. Peptides corresponding to selected sections of the primary sequence of the sodium channel, as described by Noda et al. (Nature, 312: 121-127, 1985), were synthetized. These peptides were used to identify the functional role, as well as accessibility from the external membrane surface, of the corresponding amino acid sequences of the channel molecule. This was achieved via binding experiments of the peptide to the above mAb. The peptide, which specifically binds mAb SC-72-38, was injected to rabbit to generate antibodies against the selected amino acid sequence. The antibodies thus generated were found to recognize the sodium channels of DRG cells, as evidenced by their specific modification of the voltage dependency of the steady-state channel inactivation without affecting the channel steady-state activation.

T-AM-A11   VERATRIDINE MODIFICATION OF Na CHANNELS: TRANSITIONS BETWEEN STATES. Steven Barnes and Bertil Hille, Physiology & Biophysics SJ-40, Univ. of Washington Med. School, Seattle, Wash. 98195.

Whole-cell currents through veratridine-modified Na channels in N18 neuroblastoma cells, similar to those described by this lab in frog skeletal muscle (Sutro, 1986, J. Gen. Physiol. 87:1-24, and Leibowitz et al., 1986, J. Gen. Physiol. 87:25-46), are generated in veratridine-bathed cells by trains of depolarizations that open normal Na channels. Smaller, more slowly developing inward currents are generated by sustained depolarizations. Modified current decays exponentially with $\tau = 1.25$ s at -60 mV and 23°C. Reversible closure of modified channels occurs with hyperpolarizations in the range of -110 to -180 mV, and inactivation of modified channels occurs during intense trains of depolarizations. Modification shifts the reversal potential in the negative direction.

Single channel records made with 2X normal Na concentration and 250-1000 μM veratridine in the patch electrode show that openings of modified channels (which are long and 22% of normal amplitude; inset) are usually immediately preceeded by normal openings. The 1.6 s mean burst time of modified channels (-40 mV + rest and 23°C) is interrupted by frequent 1-100 ms closings. Openings of modified channels are also seen unassociated with normal openings over a broad range of potentials and pulse paradigms as expected if there are several closed, modified states--as suggested by the whole-cell recordings. Supported by NIH grant NS08174 and a US ARO grant.
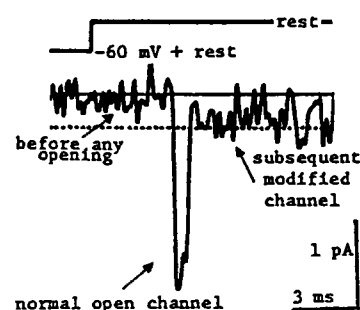
T-AM-B1 Ca^{2+} RELEASE CHANNEL FROM CARDIAC SARCOPLASMIC RETICULUM: CONDUCTANCE AND ACTIVATION BY Ca^{2+} AND ATP. ERIC ROUSSEAU and GERHARD MEISSNER   Department of Biochemistry and Nutrition, University of North Carolina, CHAPEL HILL, NC 27514

In a recent paper we have demonstrated the existence of a Ca^{2+} conducting, calcium and adenine nucleotide activated channel (Biophys. J. Nov. 1986). This Ca channel has been studied in further detail by fusing cardiac sarcoplasmic reticulum vesicles into planar lipid bilayers. The unit conductance (75 $\pm$ 3pS in 50 mM Ca^{2+} trans and 115 $\pm$ 5pS in 50 mM Ba^{2+} trans.) and the voltage dependence of the open probability (0.11/10mV for Ca^{2+} and 0.20/10mV for Ba^{2+}) were found to be dependent on the permeant ion. Single channel activity was studied in the presence of varying free cis $[Ca^{2+}]$ concentrations. An increase from 10 nM to 50 μM increased the Po in a time independent manner. Half maximum activation (P_o = 0.5 at OmV) occurred at free $[Ca^{2+}]$ = 0.7 μM and in the presence of millimolar cis ATP at $[Ca^{2+}]$ = 0.1 μM. 5 mM ATP at nM $[Ca^{2+}]$ was ineffective in activating the cardiac channel in contrast to what has been reported for the skeletal Ca^{2+} release channel. The time analysis of the open and closed events reveals that both distributions can be fit by two exponentials. The frequency and the duration of the open events increase with free $[Ca^{2+}]$ while the closed time constants decrease. ATP in the presence of Ca^{2+} has an additional effect by maintaining the channel in long open states. The different open and closed time constant values found under various activating or inactivating conditions indicate a complex gating mechanism of this multi ligand-activated channel.

T-AM-B2   THE DEPENDENCE OF THE CALCIUM TRANSIENT ON DEPOLARIZATION DURATION IN VOLTAGE-CLAMPED SINGLE HEART CELLS. J.R. Berlin, M.B. Cannell and W.J. Lederer, University of Maryland School of Medicine, Baltimore, MD 21201.

The duration of depolarization has a marked effect on tension development in voltage-clamped cardiac muscle but the changes in the underlying calcium transient have been incompletely described. We investigated the effect of depolarization duration on the calcium transient in enzymatically-dissociated rat cardiac ventricular cells voltage-clamped by a single microelectrode technique. Intracellular calcium was measured using the fluorescent calcium indicator fura-2 after injecting fura-2 into the cell from the voltage-clamp pipette. Resting calcium at a holding potential of -60 mV was 60 - 100 nM. In response to a 100 msec depolarization to 0 mV, calcium rose to a peak level of up to 1 uM within 25 - 35 msec and declined to control levels after repolarization. Shortening the depolarizing pulse (< 20 msec) reduced the peak of the calcium transient. Prolonged depolarizations did not increase the peak of the calcium transient, but revealed a decline in the level of calcium during the maintained depolarization to a level above that seen at the holding potential. During the maintained depolarization, the rate of decrease of calcium following the peak was slower than that observed after repolarization. These results suggest that, at depolarized potentials, there is a maintained net influx of calcium into the cytoplasm. This maintained influx is most likely due to a maintained release of calcium from the sarcoplasmic reticulum and/or a sustained increase in net influx by voltage-dependent sarcolemmal processes (e.g. I_{Ca} or Na-Ca exchange). Supported by NIH (HL25675) and the American and Maryland Heart Associations.

T-AM-B3   A SINGLE MODEL OF SPONTANEOUS CALCIUM RELEASE EXPLAINS CALCIUM- AND RATE-DEPENDENT SATURATION OF CONTRACTILITY, OSCILLATORY RESTITUTION OF CONTRACTILITY AND AFTERCONTRACTIONS IN HEART MUSCLE. Michael D. Stern, Maurizio C. Capogrossi, Edward G. Lakatta, Intr. by William B. Guggino. NIA and Johns Hopkins Medical Institutions, Baltimore, MD

In single cardiac myocytes, spontaneous Ca^{2+} release from the sarcoplasmic reticulum can occur between stimuli, and limit time- and Ca^{2+}-dependent restitution of twitch contractility (C). To determine the effect of this in whole muscle, we modeled the C of an ensemble of cells. Intracellular Ca^{2+} stores are released by a twitch, and reloaded mono-exponentially, approaching an asymptotic level proportional to extracellular $[Ca^{2+}]$ (Ca_o). If the stores exceed a threshold, spontaneous release occurs. Cells show spontaneous Ca^{2+}-dependent relaxation oscillations if unstimulated, provided Ca_o is above a threshold, as observed experimentally. The intercellular variability of oscillation periods was modeled by assuming that the Ca^{2+} release thresholds are distributed about a mean. We obtained analytical expressions for the mean Ca^{2+} releaseable by a stimulus (a surrogate for twitch C), and for the mean rate of spontaneous releases (a surrogate for Ca^{2+}-dependent diastolic tone). The model predicts: (1) contractility increases with Ca_o to a maximum, and then declines; (2) the Ca_o at which max C occurs increases with rate of stimulation; (3) restitution of C is damped-oscillatory at high Ca_o; (4) Ca^{2+}-dependent diastolic force is abolished immediately after the twitch (hyper-relaxation); (5) restitution of diastolic force is monophasic in low Ca_o but forms a series of damped aftercontractions in high Ca_o lagging about 90 degrees in phase behind C. Thus these experimentally observed properties of whole muscle can be explained by asynchronous spontaneous Ca^{2+} release among individual myocytes.

T-AM-B4   RYANODINE ACCELERATES CALCIUM DEPLETION FROM JUNCTIONAL SARCOPLASMIC RETICULUM OF RESTING MYOCARDIUM: AN ELECTRON PROBE STUDY. Ellyn S. Wheeler-Clark and John McD. Tormey, Dept. of Physiology, University of California, Los Angeles, CA 90024.

Ryanodine inhibits Ca release from the sarcoplasmic reticulum (SR) (A. Fabiato, Fed. Proc. 44:2970-2976, 1985), but its in situ mechanism of action is not well understood. We recently reported using electron probe x-ray microanalysis (EPMA) to measure calcium associated with the sarcolemma (SL) and junctional SR (JSR) in freeze-dried sections of rabbit papillary muscle (Wheeler-Clark & Tormey, Circ. Res. In Press, 1986). In the presence of low Na_o, contractility increased and [Ca] doubled at both the JSR and SL. Because ryanodine interacts specifically with JSR (Jones & Cala, J. Biol. Chem. $\underline{256}$; 11809-11818, 1981), we used EPMA to measure its effect on JSR and SL Ca levels. Ryanodine (10^{-6}M) was added to low Na-perfused rabbit papillary muscles to determine the proportion of low Na-induced inotropy which could be attributed to JSR Ca release. After 30 min, ryanodine had decreased developed tension to less than control (normal Na_o) levels. These muscles, when frozen after a 30 sec rest from stimulation, had JSR [Ca] below control and significantly below low Na_o values. However, SL [Ca] was still elevated. These data demonstrate 3 useful points: (1) Ryanodine (10^{-6}M), lowers in situ JSR Ca during rest, without effect on SL Ca, (2) JSR Ca content correlates better with post-rest contractility than SL Ca levels and (3) we can distinguish JSR and SL using EPMA, although JSR and SL are closely associated in situ. Application of spatial deconvolution techniques (Tormey & Wheeler-Clark, Proc NY Acad Sci, In Press, 1986) indicates that JSR [Ca] may approach zero (mmol/kg dry wt) with exposure to ryanodine. (Supported by AHA Fellowship and NIH HL31249).

T-AM-B5 Ca^{++} CURRENTS AND INTRACELLULAR Ca^{++} CONCENTRATIONS IN SINGLE SKELETAL MUSCLE FIBERS OF THE FROG. G. Brum, E. Stefani and E. Rios. Department of Physiology, Rush University, Chicago, Ill. 60612, Department of Physiology, Centro de Investigación y de Estudios Avanzados IPN, México, D.F. 07000 and Department of Biophysics, Facultad de Medicina, Montevideo, Uruguay.

The relationship between Ca^{++} current amplitudes and myoplasmic Ca^{++} transients was studied in single muscle fibers. Segments of muscle fibers were voltage clamped in a double vaseline gap chamber. Ca^{++} transients were measured as an optical signal derived from the interaction between Ca^{++} and the dye antipyrylazo III. The cells were maintained at -90 mV. Ca^{++} currents were detected at -50 mV. The peak value reached a maximum at 0 mV, thereafter it was reduced in size for larger depolarizations. The current reversed at about 40 mV. Ca^{++} transients were also detected at -50 mV and progressively increased in size with larger pulse potentials up to 10 mV. Depolarizations to voltages greater than 10 mV did not further increase the size of the transients, even though Ca^{++} currents were reduced. The magnitude and time course of transients from 10 mV to 70 mV were almost identical. Ca^{++} input fluxes were calculated from the Ca^{++} transients applying a removal model. The size of the input fluxes increased with depolarization up to 0 mV. Between 0 and 70 mV the peak input flux slightly increased while the flux measured at 200 msec remain unchanged. In conclusion, Ca^{++} transients and input fluxes are not reduced during pulses to large positive potentials, even though a drastic reduction of Ca^{++} current occures at these potentials. These observations make very unlikely that a voltage dependent Ca^{++} entry is the triggering signal for contraction.

T-AM-B6   SELECTIVITY OF THE IN SITU K CHANNEL OF FROG SARCOPLASMIC RETICULUM TO SMALL MONOVALENT CATIONS. Carla W. Abramcheck and Philip M. Best, Department of Physiology and Biophysics, University of Illinois, Urbana, IL 61801.

Replacement of K and Na with the impermeant ion choline causes a concentration dependent decrease in Ca release rate in single skinned (sarcolemma removed) skeletal muscle fibers. The ability of other monovalent cations to effect Ca release was then studied. Ca release was monitored optically using 0.5mM antipyrylazo III. Solutions contained approximately 110mM monovalent cations, 1mM Mg, 2mM MgATP, 15mM creatine phosphate, 2mM EGTA (pCa=8), and about 35mM MOPS buffer (pH=7 at 10°C), I=0.15. The concentration of highly permeable monovalent anions was limited (7mM total Cl) by using propionate salts. Following a standard loading procedure sarcoplasmic reticulum (SR) Ca release was stimulated by exposing fibers to 5mM caffeine. Changes in dye absorption (720-790nm) were monitored and analyzed by computer. The initial rate of absorption change was determined for three successive releases (control, test, control) from individual fibers. The test release rate was compared to the averaged control rates. Release rates from solutions containing 93mM K and 17mM Na were compared to those with 93mM Na and 17mM K. Release rates from the high Na solutions were 101±5 percent (mean± SE)(n=4) of those in the high K solutions. Therefore Na was considered as conductive as K. Substitution of various monovalent cations for 50% of the K and Na concentration gave the following percent of control Ca release rates (mean±SE): Rb 96±6 (n=6), Li 83±2 (n=7), Cs 81±8 (n=6). The effect on Ca release rate should vary with the relative conductance of the SR K channel for the substituted ion. Our results suggest that the relative selectivity of the in situ SR K channel is K = Na = Rb > Li = Cs >> choline.   Supported by NIH AR 32062, MDA, and PHS Training Grant GM7143.

T-AM-B7   MYOPLASMIC CALCIUM TRANSIENTS MONITORED SIMULTANEOUSLY WITH HIGH AND LOW AFFINITY
CALCIUM INDICATORS.   M.G.Klein, B.J.Simon, G.Szucs and M.F.Schneider, Dept. of
Biological Chemistry, University of Maryland School of Medicine, Baltimore, MD 21201 USA
     Isolated frog skeletal muscle fibers cut at both ends were voltage clamped (6-8° C) in a
double vaseline gap chamber with end pools containing the relatively high affinity Ca indicator
fura-2 (50 μM) and the lower affinity antipyrylazo III (AP III; 1 mM). The fiber in the central
pool was trans-illuminated (650-900 nm) by light from a tungsten halogen source and
epi-illuminated (380,355-360 or 350 nm) by a xenon source. Using dichroic mirrors of
successively longer wavelengths, each followed by an appropriate filter and photodiode, the
fluorescence at 510 nm (fura-2) and the transmittances at 700 nm (AP III plus intrinsic signal)
and 850 nm (pure intrinsic) were monitored simultaneously. As pulse amplitude and/or duration
were increased the fura signal clearly saturated when the AP III signal was still increasing.
For pulses well below fura saturation the fura signal decayed considerably more slowly than the
AP III calcium transient. Thus AP III appears preferable to fura-2 for large or fast calcium
transients whereas fura-2 can be used for monitoring relatively slower changes in calcium or
resting levels that cannot be accurately determined by AP III. Using 380 nm illumination the
fura signal exhibited a very slow (10s of s) phase of decay following repolarization. The size
of this slow component increased with the amplitude and/or duration of the preceding pulse. At
the isosbestic wavelength for Ca-fura (∿358 nm) no signal was seen. Since fura-2 is insensitive
to pH and Mg-fura gives a larger signal at 358 nm than at 380 nm (Grynkiewicz et al., 1985) the
slow 380 nm fura signal probably represents a true slow phase in the decay of calcium.

T-AM-B8   NEOMYCIN BLOCKS ASYMMETRIC CHARGE MOVEMENTS AND CA TRANSIENTS IN SKELETAL MUSCLE FIBERS.
J. Vergara, Department of Physiology, UCLA, Los Angeles, CA 90024.
     An important evidence in support of the possible involvement of inositol 1,4,5-trisphosphate
as a chemical link in excitation-contraction coupling in skeletal muscle came from experiments
showing that neomycin blocks the Ca transients recorded in fibers electrically stimulated to elicit
action potentials (Vergara et al., PNAS, 82:6352,1985). Neomycin is a polycationic antibiotic
which binds tightly to polyphosphoinositides and prevents their enzymatic degradation (Schacht,
J.Neurochem., 27:1119,1976). I have further investigated the effects of this drug on Ca transients
and asymmetric charge movements (Schneider & Chandler, Nature, 242:244,1973) recorded from frog
single muscle fibers voltage-clamped with the three vaseline gap method. The fibers were internally
diffused with Cs containing relaxing solutions to which the Ca indicating dye Azol was added, and
externally perfused with saline containing TEA, Ca, SO_4, MOPS, and TTX. Neomycin (0.3-1 mM) was
added to the internal solutions at the pools where the fiber ends were cut. After a period of 30-50
minutes required for diffusion of the drug from the cut ends, it was observed that the Ca
transients diminished in amplitude and rate of rise, and simultaneously, the asymmetric charge
movements decreased in size. The effect progressed towards the abolition of both the Ca transients
and the charge movements. The total membrane capacitance was not significantly reduced by neomycin,
indicating a good preservation of the T-system structures. These results give support to a possible
interpretation of the asymmetric charge movements recorded in skeletal muscle fibers as an effect
of the dynamic alteration in the phosphoinositides' contents of the T-system membranes in response
to electrical stimulation. Supported by grants from MDA and USPHS (AM25201).

T-AM-B9   THE EFFECT OF PHENYLEPHRINE ON CALCIUM CURRENT IN ISOLATED ADULT FELINE MYOCYTES. H.A.
        Hartmann and S. R. Houser. Department of Physiology Temple University School of Medicine
     Philadelphia, PA 19140
     Previous studies have shown that stimulation of the alpha-1 receptors results in an elevation of
intracellular calcium. This result is thought to occur via an inositol triphosphate mediated
release of calcium from intracellular stores. To date, however, the possibility that alpha-1 stim-
ulation results in an increase in calcium influx through voltage dependent membrane channels has not
been evaluated. The objective of the present research was to determine if alpha-1 stimulation has
a direct effect on voltage dependent calcium channels. This potential role of alpha-1 receptor
stimulation was investigated in enzymatically dissociated adult feline ventricular myocytes. To
eliminate sodium currents, myocytes were superfused with a zero sodium, 140 mM TEA solution con-
taining 5 mM calcium. Myocyte voltage was controlled with a single electrode whole cell voltage
clamp technique using suction type pipettes containing 120 mM CsCl to block potassium currents and
10 mM EGTA. Myocytes were held at -80 mV and stepped for 500 msec (0.5 Hz) to + 10 mV. Exposure
to 0.1 mM phenylephrine produced a 61% increase in peak inward current at + 10 mV. However, when
the experiment was repeated in the presence of 1 x 10-6 M propranolol, the effect of phenylephrine
was not observed. Theses findings suggest that alpha-1 stimulation does not result in an increase
in calcium current in adult feline myocytes. However, it does appear that phenylephrine increases
inward calcium current through the stimulation of the beta receptor. (Supported by NIH Grants
HL 33921 and HL 33648 2SRH.)

T-AM-B10 MACROSCOPIC KINETICS OF CHLORIDE CONDUCTANCE IN FROG MUSCLE AT pH 5
Peter C. Vaughan, Dept. Physiology, University of British Columbia, Vancouver, B.C. V6T 1W5; J. Mailen Kootsey and Michael D. Feezor, Dept. Physiology, Duke University Medical Center, Durham, NC 27710.

At pH 5, the chloride conductance of frog skeletal muscle membrane increases during hyperpolarization and decreases during depolarization. The data of Loo *et al* (1) suggests that the anion conducting channel may behave as a two-state device which opens and closes with first-order kinetics. Three-microelectrode voltage clamp experiments were performed on cells depolarized and loaded with chloride to test this possibility. Clamp currents were recorded for membrane potential steps over the range $V_{rest} -120\ mV$ to $V_{rest} +70\ mV$. Ten fibers produced sufficient data for opening and closing rate constants to be fitted over the whole range, using first order precepts and assuming that the currents were recorded from membrane at uniform potential. Prior conditioning at potentials more positive or negative than the resting potential did not influence the time course of the relaxation to the steady state at the test voltage. Thus, the opening-closing mechanism appears to be first order. However, while the recorded relaxations appeared to be well fit by single exponentials, they were systematically nonlinear when plotted on a logarithmic ordinate. We simulated the voltage clamp experiment on a digital computer, representing the muscle preparation as a one-dimensional cable with membrane described by a capacitance in parallel with the first-order chloride conductance. The simulations included the clamp amplifier with finite gain and bandwidth and the resistance of the current injection electrode. The currents from the simulated experiments also showed deviations from linearity in a semi-logarithmic plot similar to those observed in the experiments. Thus we conclude that the apparent deviations from first-order behavior in the chloride conductance are probably caused by the nonuniformity of membrane potential within the experimental preparation, i.e. by errors in the approximation used in the three-electrode clamp method. (JMK and MDF supported in part by USPHS grants RR01693 and HL12157.)
1. Loo, D.D.F., McLarnon, J.G., and P.C. Vaughan, Can. J. Physiol. Pharmacol. 59:7-13, 1981)

T-AM-B11 IONIC CURRENTS IN SINGLE CELLS FROM GUINEA PIG TAENIA COLI. Y. Yamamoto, S.L. Hu, and C.Y. Kao, Department of Pharmacology, SUNY Downstate Medical Center, Brooklyn, NY 11203

Using the tight-seal patch-clamp method, whole-cell currents have been obtained from freshly collagenase-dispersed single smooth muscle cells from the guinea pig taenia coli. In Krebs' solution containing 5 mM K^+ and 1 mM Ca^{2+}, cells with -40 mV resting potentials respond to outward current steps with action potentials of ca. 60 mV; repetitively if the step is long. Membrane capacitance is about 50 pF and input resistance 1-2 Gohm; the expected membrane time-constant of ca. 100 msec closely agrees with that seen in hyperpolarizing responses.

Under voltage-clamp conditions, depolarization causes an initial inward current followed by a large outward current. The inward current is carried by Ca^{2+}, as its magnitude and reversal potential vary with $[Ca^{2+}]o$. The outward current has a gradual onset, and is well-maintained for voltage steps of 40-200 msec, but declines (inactivates) with steps of several sec. It is a K^+ current, as its reversal potential is around -65 mV, its amplitude is strongly influenced by $[Ca^{2+}]o$, and it is fully blocked by 130 mM Cs^+ internally and 30 mM TEA^+ externally. When I_K is absent, I_{Ca} can be seen to activate rapidly, peaking at 4 msec at 34°C, and to inactivate slowly with multiple exponentials, the slowest component with time-constant of about 1 sec.

The identity of the charge-carrier and their reversal potentials confirm previous conclusions from small multicellular preparations. The new kinetic findings show that substantial current overlap must exist even in single dispersed cells. (Supported by NIH grant HD00378).

T-AM-B12 SINGLE CHANNEL BASIS OF DELAYED RECTIFICATION IN DISPERSED CELLS OF GUINEA PIG TAENIA COLI. S.L. Hu, Y. Yamamoto, and C.Y. Kao, Department of Pharmacology, SUNY Downstate Medical Center, Brooklyn, NY 11203

Single-channel events have been recorded in cell-attached and inside-out patches from freshly collagenase-dispersed single smooth muscle cells of the guinea pig taenia coli. Under conditions mimicking physiological states with $[K^+]_i$=125 mM and $[K^+]_o$=5 mM, two types of channels are observed, as the steady-state holding potenial, lasting minutes, is moved from -50 mV towards the positive. The more active type with unit conductance of 175 pS first appears at ca. -30 mV; the other of 65 pS activates at ca. -20 mV. When patches held at -50 mV (which are largely quiescent) are subjected to depolarizing steps of 50 msec duration, only the 175 pS channels are observed. The probability of opening of single channels as well as the number of open channels rise with increasing depolarization. Summing 20-60 traces at each voltage step leads to current traces that closely resemble I_K seen in whole-cell recordings, including a gradual onset, a maintained magnitude, and an outward rectification. The 175 pS channel has a reversal potential of ca. -70 mV, is blocked by internal Cs^+, and its unit conductance is reduced to 35% in Rb^+. It is influenced by $[Ca^+]_i$: at pCa_i of 8, 7, and 6, unit conductance remains almost constant at 175, 170 and 167 pS, but the probability of opening rises with increasing Ca^{2+}. From these characteristics, the 175 pS unit can be identified as the delayed rectifier channel. (Supported by NIH grant HD00378).

T-AM-C1   THE PROPAGATION OF THE NERVE IMPULSE. N. Jurisic (Intr. by M. Delay).
Departamento de Fisica, Facultad de Ciencias, Universidad Central de Venezuela, Caracas, Venezuela.

A partial differential equation for the propagated action potential is derived using symmetry, charge conservation, and Ohm's law. Charge conservation analysis explicitly includes the gating charge when applied in the laboratory frame of reference. When applied in the frame of reference where the capacitive currents are zero, it yields a relation between the orthogonal components of the ionic current allowing us to express the nonlinear ionic current across the membrane in terms of the membrane capacitance and the axial current in the laboratory which satisfies Ohm's law. The ionic current is shown to behave as $[C(V)V]^2$ at the foot of the action potential, where C(V) is the voltage dependent capacitance of the membrane. Improved knowledge of the nonlinear term behavior makes possible to describe the propagated action potential in an approximated way with quasilinear partial differential equations. These equations have analytical solutions which travel with constant velocity, retain their shape and account for other properties of the action potential. Furthermore, the quasilinear aproximation is shown to be equivalent to the FitzHugh-Nagumo model without recovery.

T-AM-C2 IS THE CA^{+2}-VOLTAGE HYPOTHESIS - AN EXPERIMENTAL ARTEFACT?
I. Parnas and H. Parnas, Neurobiology, The Hebrew University, Jerusalem.

The Ca-voltage hypothesis for neurotransmitter release suggests that depolarization, in addition to increasing membrane conductance to Ca^{+2}, activates a membrane molecule S. The activated S binds Ca^{+2} to form a complex CaS initiating the chain of processes leading to release. Thus Ca^{+2} is essential, but insufficient for phasic release. Moreover, the time course of S formation and inactivation controls the kinetics of release. This hypothesis is supported by several lines of experiments: (1) At high depolarizations, release is higher even though the concomitant entry of Ca^{+2} is lower. (2) A small test pulse which is insufficient to produce release, when given after a train of impulses, increasing [Ca]i, produces a large release. (3) Release is reduced by a hyperpolarizing pre or post pulse. (4) Kinetics of release is independent of changes in Ca^{+2}, but is modulated by a hyperpolarizing post pulse. Recently, Zucker and Landò challenged results 1 and 2. They claim result (1) is due to an uneven depolarization below the Lumen and the rim of the electrode and result (2) is due to changes in terminal excitability, the train causing the subthreshold test pulse to become superthreshold. We refute this criticism by showing that result (1) can be repeated with intracellular terminal depolarization (Parnas, Parnas, Atwood and Wojtowicz). The "rim artefact" obviously does not exist under this condition. We have repeated experiment (2) in TTX, thus avoiding the problem of changes in excitability. We also find that quantum size remains constant at higher depolarizations, excluding the possibility of recruitment of release sites below the rim.

T-AM-C3 ON THE LATENCY SHIFT IN NEUROTRANSMITTER RELEASE
H. Parnas, I. Parnas, H. L. Atwood and M. Wojtowic. Neurobiology, Hebrew Univ. Jerusalem and Physiology, Univ. of Toronto, Toronto.

Release of neurotransmitter has been shown to be delayed upon prolongation of the depolarizing pulse. This latency shift has been observed at low, moderate and high depolarizations. At the strong depolarizations, the delay shift has been attributed to suppression of calcium entry during the pulse. This explanation cannot however hold for depolarizations below the suppression potential for calcium entry. Theories suggesting that depolarization depresses release, were therefore advanced. In the present work, we reinvestigated the problem of delay shift at low and moderate depolarizations. Using extracellular "macropatch" technique or an intracellular electrode in the nerve terminal of crayfish and lobster, we find that at low and moderate depolarization, release starts with the same minimal delay irrespective of pulse duration. Our results differ from those previously published because a) the same number of pulses is given at the different pulse durations, b) synaptic delay histograms are not normalized. Under these conditions the minimal delay is independent of pulse duration and only the peak of the delay histogram is shifted to the right at longer depolarizations. Our results suggest that there is no need to postulate a suppressive role for membrane depolarization in release.

T-AM-C4 EXPLANATION OF HEAT BLOCK AND COLD BLOCK BY THE FERROELECTRIC ELECTRODIFFUSION
MODEL. H. Richard Leuchtag, Department of Biology, Texas Southern University, Houston, TX 77004.

The ferroelectric electrodiffusion model (Biophys. J. 49:410a) is a modification of classical
electrodiffusion with the assumption of a linear channel dielectric replaced by a nonlinear
relationship between electric field and electric displacement. This model predicts the existence
of spontaneous polarization reversible by an applied electric field, i. e., ferroelectricity.
One of the implications of the hypothesis that the Na channel contains a ferroelectric unit is
the existence of a transition temperature above which the spontaneous polarization disappears,
the (upper) Curie point. If the spontaneous polarization of the ferroelectric channel unit is
necessary to excitability, manifestations of excitability such as axonal conduction must be
abolished at this temperature. This phenomenon (heat block) has been observed, along with the
phenomenon of cold block, a lower limit to excitability (see e. g. Chapman, Nature 213:1143,
1967). Cold block also is explainable by the ferroelectric electrodiffusion model, in that a
number of ferroelectrics (such as Rochelle salt) exhibit a temperature (the lower Curie point)
below which spontaneous polarization disappears. The Curie-Weiss law, $\epsilon_c = C/(T - T_c)$,
derivable from this model, predicts that the dielectric permittivity, ϵ_c, approaches infinity at
the Curie points T_c. Such an anomaly has been observed in the membrane capacitance of <u>Loligo</u>
<u>pealei</u>, which increases steeply with temperature above 42 $^{\circ}$C (Palti & Adelman, J. Memb. Biol.
1:431, 1969).

T-AM-C5 EQUIVALENCES AND DIFFERENCES OF BLEACHING AND BACKGROUND ADAPTATION IN VERTEBRATE RODS.
K.N. Leibovic, Y.Y. Kim, Z.H. Pan, Department of Biophysics, SUNY/Buffalo.
There is an extensive literature on visual threshold as a function of light adaptation. Other
response parameters, however, have not been studied as well. From recent work it has become
increasingly clear that visual adaptation is mediated primarily in photoreceptors.
By using intracellular recordings in Bufo rods we have shown that the relationship between
bleaching and backgrounds at threshold extends to the complete response range. Thus, one can
establish a unique equivalence between light and bleaching with respect to response compression and
shift of the operating range. At first sight this might suggest that light and bleaching operate
through a common mechanism. But this is not so. For, the response kinetics are quite different in
the two cases. We have demonstrated this for response activation and inactivation and for the
shapes of the response waveforms. Consequently, the equivalence between light backgrounds and
bleaching for peak responses does not extend to the response kinetics.
Our results have interesting implications for psychophysics. Thus, the form we have observed
for response activation is related to Bloch's law of stimulus summation; inactivation is related to
recovery of sensitivity; and the equivalence between bleaching and light backgrounds with respect
to the peak responses implies that the latter mediate brightness perception. This last statement
is based (i) on the result that a bleached retinal area appears equally bright as an illuminated
area if the two have the same threshold elevation, and (ii) on the nonequivalence of the response
waveforms except at the peak of the response.
Supported by NEI grant R01 EY0 3672.

T-AM-C6 SYNAPTIC ACTIVITY-DEPENDENT CALCIUM SEQUESTRATION IN PURKINJE CELL SPINE ORGANELLES.
S.B. Andrews*, R.D. Leapman#, D.M.D. Landis¶ and T. S. Reese*§, NINCDS* and BEIB#, NIH, Bethesda,
MD, Case-Western Reserve University¶ and Marine Biological Laboratory§, Woods Hole, MA.
One hypothesis for the regulation of synaptic plasticity and potentiation in dendritic spines
invokes Ca influx through activated channels to modulate the metabolic state of the spine. The
presence of Ca-sequestering organelles--perhaps smooth-endoplasmic reticulum (SER) whose function is
to buffer cell Ca to activating levels--is a likely corollary of this hypothesis. Here we report
the first direct evidence for Ca sequestration by the SER cisterns of Purkinje cell dendritic
spines, and further show that this sequestration is dependent on synaptic activity. A slab of
cerebellar cortex containing undamaged parallel fiber/Purkinje cell synapses from 40d old mice was
obtained by quick excision, and directly frozen within 20-30s. Cryoultramicrotomy, cryotransfer,
low-temperature electron microscopy and electron probe analysis were used to identify and to deter-
mine the elemental content of synaptic structures. Such experiments showed a bimodal distribution
of total Ca within spine cisterns, with population means of 1.4±0.4 and 8.2±0.7 mmol/kg dry wt.
These populations are thought to represent resting and activated spines, respectively. This inter-
pretation is supported by experiments on brain slices which were incubated in an oxygenated Ringer
for 2h, followed by direct freezing either with or without K depolarization. The Ca content of
spine cisterns in resting synapses (1.2±0.4 mmol/kg) was similar to the low-Ca population of fresh
spines, while that of depolarized slices was greater than the high-Ca group from fresh brain. These
results imply that the cytoplasmic Ca of dendritic spines is indeed raised following depolarization,
and that the formerly extracellular Ca accumulates within SER.

T-AM-C7   INTRACELLULAR STUDIES OF REACTIVE GLIA IN RAT HIPPOCAMPUS. Dennis J. McFarland[1], Charles
Bowman[2], Harold K. Kimelberg[3], and John W. Swann[1]. 1. Wadsworth Center for Laboratories
and Research, NYS Department of Health, Albany, NY 12201. 2. Department of Biophysics, University at
Buffalo, Buffalo, NY 14214. 3. Albany Medical College, Albany, NY 12209.

We are investigating the reactive gliosis that occurs one month after stereotaxic directed micro-
injection of kainic acid (4 nmol) into the CA3 region of the dorsal hippocampus of the rat. In
general, virtually all of the pyramidal cells of the CA3 subfield were destroyed by the kainate, and
varying degrees of cell loss occurred in the other classes of neurons in this region as well. An
increase in the density of GFAP positive elements, and in particular, their size, was also observed
in the kainate treated hippocamppi. In contrast to the neurons in the normal hippocampal slice, the
membrane potentials of the majority of the cells in the treated slices were -77 ± 7 mV (130 cells),
with a smaller number of cells having a membrane potential of -52 ± 5 mV (27 cells). The membrane
potential of the lower potential cells decayed within a few minutes (25 cells), but 2 cells
maintained their membrane potential and showed endogenous electical activity. By contrast, 66 cells
(out of 130 cells) with the higher membrane potential had stable potentials over the same time
period, appeared electrically unresponsive, and appeared to have a very low input impedence. The
membrane potential of the higher potential cells responded to increases in K^+ above 5 mM, and had
a slope of approximately 55 mV per decade change. Ionophoresis of glutamate depolarized the membrane
potential of some, but not all cells.

Supported by NIH grants: NS 18309 to JWS, NS 24891 to CLB, and NS 19492 to HKK.

T-AM-C8   SPATIAL DISTRIBUTION OF ION CHANNELS IN HAIR CELLS OF THE BULLFROG'S SACCULUS.
W. M. Roberts and A. J. Hudspeth, Department of Physiology, University of California, San Francisco,
CA 94143-0444.

Hair cells are the sensory receptors in vertebrate auditory and vestibular systems. In addition to
mechanosensitive channels in their stereocilia, hair cells of the frog's sacculus possess Ca and K_{Ca} channels
that are involved in frequency tuning by electrical resonance; Ca channels are also expected to occur at
presynaptic sites on the basolateral surface. The goal of these experiments was to determine the spatial
distribution of these ion channels. Hair cells were isolated from Rana pipiens by papain digestion. We used
loose-seal pipettes to record from patches covering 5-80% of each cell's surface; membrane capacitance was
used to estimate the membrane area under the electrode. A separate, tight-seal pipette controlled the
intracellular potential and recorded the whole-cell current. Depolarization from -70 to -10 mV evoked a
biphasic, whole-cell current that was the sum of an inward Ca current and an outward K_{Ca} current; the steady-
state outward-current density was 1.4 ± 0.6 pA/μm^2 (mean$\pm$S.D., n=16). The current in basolateral patches
followed a timecourse similar to that of the whole-cell current. Both Ca and K_{Ca} channels were distributed
widely in the basolateral region of the cell; patch-current densities were 0.6-3.2 pA/μm^2 (mean=1.7; S.D.=0.9;
n=12). No voltage-gated channels were present on the apical surface, supporting previous evidence that the
transduction channels are not significantly voltage-sensitive. Pipettes that covered entire apical surfaces,
including hair bundles, recorded capacitances of 2.5-5.0 pF, consistent with the surface area estimated from
morphological data. Supported by NIH grants NS07904 and NS22389.

T-AM-C9   **BROWNIAN MOTION OF HAIR BUNDLES FROM THE FROG'S INNER EAR**. J. Howard and A. J.
Hudspeth (Introduced by Evelyn Ralston) Department of Physiology, University of
California, San Francisco, CA 94143-0444.

Hair cells, the sensory receptors of the ear, respond electrically when their hair bundles are
deflected by forces that originate from external stimuli such as sound or acceleration. Hair
bundles are also subject to thermal forces; the resulting Brownian motion, which may set an ulti-
mate limitation on sensitivity, is determined by the viscoelastic properties of and hydrodynamic
damping on the hair bundle. We measured the stiffness and spontaneous motion of individual saccu-
lar hair bundles by attaching to each bundle's tip a flexible glass fiber whose position was
monitored optically. In eight cells, the power spectrum of the bundle's spontaneous motion was
the sum of two Lorenzians with corner frequencies 9 ± 3 and 470 ± 120 Hz and amplitudes $0.12 \pm .06$ and
0.006 ± 0.002 nm^2/Hz respectively; the errors are standard deviations. The spontaneous motion was
consistent with the Brownian motion of a mechanical network comprising the following three sets of
elements in parallel: 1) a spring (0.43 mN/m); 2) a spring (0.22 mN/m) in series with a dashpot
(3.5 μN·s/m); and 3) a dashpot (0.18 μN·s/m). This confirms our previous observation that the
bundle behaves mechanically like a Maxwell element [the combination of elements 1) and 2)]. The
third element evidently includes damping from the fluid and frictional damping within the bundle.
Two cells showed, in addition, active motion: their bundles resonated at about 100 Hz in response
to force steps and their spontaneous motion exceeded that expected from Brownian motion alone.
Supported by NIH grant NS20429 and by the System Development Foundation.

T-AM-C10   ELECTRICAL ACTIVITY IN HOLOTHURIAN MUSCLE. Robert B. Hill, Department of Zoology, University of Rhode Island, Kingston, R.I. 02881

Spontaneous contractions of a segment of isolated muscle of <u>Holothuria</u> <u>cinerascens</u> begin with asynchronous spiking and a gradual depolarization. The time course of the depolarization, which underlies the spiking, is parallel to the time course of the subsequent contraction. Bursts of large spikes precede a rapid phase of contraction. Spontaneous contractions are not propagated across a sucrose gap. Caffeine contractures are not accompanied by depolarization, and contractility is lost in a series of caffeine contractures. Depolarization with KCl temporarily restores the contractility lost in a series of caffeine contractures. Both acetylcholine and KCl induce overall depolarization and correlated force, but in low concentrations of acetylcholine individual muscle units may depolarize independently, perhaps indicating differing sensitivities.

T-AM-C11   OLIGODENDROCYTE PLASMA MEMBRANE: RELATION TO MYELIN. S. Szuchet, P.E. Polak, S.H. Yim, and D. Arvanitis, Department of Neurology and The Brain Research Institute, The University of Chicago, Chicago, IL 60637.

Although myelin is an extension of oligodendrocyte (OLG) plasma membrane (PM), it is not known if the two membranes resemble one another. Structurally myelin is complex, but its protein composition is simple: two proteins, proteolipid protein (PLP) and basic protein (MBP), constitute ~80% of the total. Other proteins are 2',3', cyclic nucleotide phosphodiesterase (CNPase), a glycoprotein (MAG) and DM-20. We have developed procedures for isolating and purifying OLG-PM to high purity and found that OLG-PM may contain structural and functional(?) domains that differ in lipid:protein and cholesterol:phospholipid ratios. The protein profiles of these subfractions exhibit only quantitative differences. Comparison of the protein profiles of PM and myelin shows that they are distinct. But similarities also exist. Notably, they share a group of 4 bands, M_r=43K-58K. These bands correspond to CNPase, tubulin and possibly actin. Other common components have M_r=140K-220K. PLP and MBP, M_r=24K and 18K, respectively, are not present in OLG-PM or are minor components. To investigate this point, we labeled cells with precursors prior to PM purification, resolved the proteins on SDS-PAGE, transferred onto nitrocellulose, stained the strips with specific antibodies against PLP, MBP, DM-20, MAG and exposed the strips to X-ray film. These experiments showed that OLG-PM contains: a) PLP and DM-20 as minor components; b) MAG as a major glycoprotein; and c) no MBP. These results were confirmed by immunostaining intact cells at the EM level. Taken together our data show that myelin is not a simple extension of OLG-PM but is selectively enriched in certain proteins. Supported by Natl. MS Soc. grant RG-1223-C4.

T-AM-C12   VARIATION OF ACETYLCHOLINE RECEPTOR CHANNEL KINETICS WITH AGONIST CONCENTRATION IN CULTURED MOUSE MUSCLE, Meyer B. Jackson, Department of Biology, University of California, Los Angeles. The patch clamp technique was used to study the gating kinetics of the acetylcholine receptor with the concentration of the agonist carbamylcholine varying from .25 to 10.0 μM. Data in which many channels were often open at the same time were analyzed with the aid of mathematical expressions that relate the stochastic behavior of a many channel system to the stochastic behavior of a single channel (Jackson, M.B., Biophys. J. <u>47</u>:129-137, 1985). Analysis of data by these methods is shown to provide reliable estimates of parameters. Single-channel open-time densities are best described by a sum of two exponentials. The fraction of slowly closing channels increased linearly with agonist concentration, in a manner consistent with the opening of singly and doubly liganded receptor channels. The time constant of the slow component in the open-time density increased slightly with agonist concentration, suggesting slow block of the channel by agonist. The time constant of the fast component did not exhibit detectable variation with agonist concentration, because this process is too fast to be noticeably altered by slow channel blockade.   At .25 μM carbamylcholine the frequency at which openings were observed was only about twice the background frequency of spontaneous opening. At 10.0 μM carbamylcholine, immediately after seal formation and before the onset of desensitization, the frequency of opening was approximately 300 times higher.   The frequency of brief duration openings showed an approximately linear increase with agonist concentration, while the frequency of long duration openings increased approximately as the square of the agonist concentration.

T-AM-D1 INTERACTIONS OF DEFINED MEMBRANE SURFACES WITH AQUEOUS TWO PHASE POLYMER TEST SYSTEMS
J.F. Boyce and D.E. Brooks, Departments of Pathology and Chemistry, University of British Columbia, Vancouver, Canada, V6T 1W5.

Cell membranes generally bear a layer of glycoprotein and glycolipid on their external surface, the glycocalyx, which contains ionic groups distributed throughout its depth. Cellular interactions depend largely on the structure and reactivity of the glycocalyx yet very little is known about its depth, density, the distribution of charge and mass throughout the region, and the effect of changes in these parameters on the cell's interaction with its environment. Partition in aqueous two phase polymer systems has been shown to be a sensitive technique for detecting alterations in the glycocalyx of cells but it is difficult to interpret analytically. We have exploited the sensitivity of the aqueous polymer system to develop a simplified experimental model of the cell surface which permits the thickness, density, and charge distribution of the glycocalyx to be manipulated. Monolayers of lipids and glycolipids are formed on a dense fluorocarbon liquid substrate under one phase of an aqueous two polymer phase system. The molecular packing and surface charge density can be adjusted by compressing or expanding the film while the free energy of the interface is monitored by measuring the contact angle of a test droplet of the second phase resting on the lipid surface. The characteristics of the layer are determined by the nature of the glycolipids chosen. Using aqueous polymer systems bearing known differences in electrostatic potential between the phases and substrates of known charge distribution we have found that existing electrostatic theories do not predict the dependence of contact angle on charge density of the surfaces. (Supported by the Medical Research Council and the Canadian Heart Foundation).

T-AM-D2

SYNCHROTRON X-RAY DIFFRACTION AND REFLECTION STUDIES OF PHOSPHOLIPID MONOLAYERS AT THE AIR/WATER INTERFACE. C.A. Helm, L.A. Laxhuber, H. Möhwald, TU Munich Physics Dept. E 22, D-8046 Garching, K.. Kjaer, J. Als-Nielsen, Riso Natl.Lab., DK-4000 Roskilde.

Monolayers of the pospholipid L-α- dimyristoylphosphatidic acid (DMPA) are studied by Synchrotron X-ray diffraction and reflection varying surface pressure and charge density. It is shown that, increasing the pressure above the value π_c distinguished by a break in the slope of the pressure area isotherm, a phase with short range positional order is formed. This phase undergoes a transition to a positionally ordered solid phase at a distinct pressure π_s which is more than 10 mN/m larger than π_c. Hence condensed phase domains formed at pressures corresponding to the nearly horizontal part of the pressure/area isotherm exhibit positional disorder, but, according to electron diffraction and fluorescence polarization studies, orientational order over distances of μm. The positional order coherence length in the solid phase amounts to about 100 lattice spacings.
Measurements of X-ray reflectivity as a function of incidence angle can be interpreted within a simple model. This shows that a decrease in molecular density leads to a reduction of thickness as well as density in the hydrocarbon layer. Supported by the German Bundesministerium für Forschung und Technologie and by the Danish National Science Foundation.

T-AM-D3 TRANSFER OF LONG CHAIN FLUORESCENT FATTY ACIDS FROM DMPC TO EGG PC VESICLES. Judith Storch and Alan M. Kleinfeld. Dept. of Physiology and Biophysics, Harvard Medical School, Boston, MA 02115
In an effort to determine the factors governing transport of of long chain free fatty acids (lcffa) across membranes we have recently studied the transfer of fluorescent analogs, the n-(9-anthroyloxy)ffa (n-AOffa), between small unilamellar vesicles composed of egg phosphatidylcholine (PC), at 24°C (Storch and Kleinfeld, (1986) Biochemistry 25:1717). This study showed that transfer of 12-AO-sterate (12-AS) involves two rates (in (min)$^{-1}$): transbilayer flip-flop (0.35), which is rate limiting, and transfer from the vesicle into the aqueous phase (k_{off}=2.3). We have now used this same methodology to study transfer of 12-AS from donor SUV composed of dimyristoyl PC (DMPC). The results of this study are surprising on two accounts. First, at temperatures below the phase transition (24°C), transfer again involves two rates, although both of these are about 3 fold slower than for egg PC. In addition, these rates are relatively temperature insensitive in the range 5°C to 24°C. Second, and most important, at temperatures above the phase transition the transfer is best described by a single rate. This rate is k_{off}, and increases from .8 to 2.6 in the temperature range 30°C to 45°C. Thus, while the rate of flip-flop is limiting in egg PC (fluid state) and gel state DMPC, it is not rate limiting in fluid state DMPC. This result indicates, therefore, that relatively subtle changes in the lipid composition of membranes can change the mechanism of lcffa transport across membranes. Supported by AHA grants 86-1253 and 82-174.

T-AM-D4   NMR STUDIES OF THE INTERACTIONS OF LPS IN PE VESICLES WITH METAL CATIONS AND POLYMYXIN B.
H.D. Dettman and I.M. Armitage, Dept. of M.B. and B., Yale Univ., New Haven, CT 06510.

The outer membrane of gram negative bacteria protects the organism from many lipophilic drugs and detergents. Lipopolysaccharide (LPS), a major component of the outer membrane, plays a key role in determining the integrity of this "barrier-function": the interaction of LPS with inorganic cations (ie. Mg^{2+}, Ca^{2+}) stabilizes the outer membrane while organic cations, such as the antibiotic, polymyxin B, cause disruption. We have used nuclear magnetic resonance (NMR) techniques to study the effects of multivalent cations on the LPS isolated from the E. coli K12 heptoseless mutant, D21f2, reconstituted into E. coli phosphatidylethanolamine (PE) vesicles. The structure of this LPS consists of Lipid A (a diglucosamine moiety, substituted with N- and O-linked fatty acyl-chains and mono- and/or di-phosphate groups) and two molecules of 2-keto-3-deoxy-D-manno-octulosonic acid (KDO) in the core sugar region. ^{31}P NMR has shown that the phosphate groups bind metal ions [Strain et al (1983) J. Biol. Chem. 258, 13466]; ^{23}Na NMR studies of linewidth versus pH suggest that the KDO carboxyl groups are also involved [Strain, Dettman and Armitage, to be published]. LPS/PE vesicles have been used for competitive titrations between Na^+ and Mg^{2+}, Ca^{2+} or polymyxin B, monitored using ^{23}Na NMR; the dissociation constant (K_d) for each of the cations has been determined. The interaction of polymyxin B with LPS was studied further with LPS containing deuterated acyl-chains (^2H-LPS); ^2H NMR has shown that the titration of LPS/PE multilamellar vesicles with polymyxin B causes an increase in LPS fatty acyl-chain fluidity, similar to that obtained with increasing temperature. These experiments have given insight as to the mechanism by which Mg^{2+} and Ca^{2+} stabilize and polymyxin B destabilizes bacterial outer membranes. (Supported by NIH grant # AI20984).

T-AM-D5   INFLUENCE OF MEMBRANE LIPID COMPOSITION ON TRANSLOCATION OF NASCENT PROTEINS IN HEATED

E. COLI. Milton B. Yatvin, University of Wisconsin Clinical Cancer Center, Department of Human Oncology, Madison, WI 53792.

In studies using Escherichia coli we have shown that new protein species appear in the outer membrane fraction with concomitant losses of nascent proteins from the soluble and inner membrane fractions following heat exposure. Of the various explanations for this phenomena, temperature-induced membrane disorganization appeared the most likely to account for the observed flow of the majority of newly synthesized proteins to the outer membrane. To test this hypothesis we grew E. coli K1060 cells, an unsaturated fatty acid requiring auxotroph, supplemented during growth with fatty acids of varying chain length in an attempt to determine whether biological membranes of varying ability to maintain their bilayer configuration could be constructed. The rationale being that such membranes would allow us to determine whether translocation would occur differently in cells grown at the same temperature supplemented with either 16:1 or 20:1 unsaturated fatty acids when the cells were subjected to a series of thermal insults. Protein translocation occurred to a greater extent and at lower temperatures in cells supplemented with the longer chain fatty acid. Based on treatment of outer membranes with either 1 M salt, 6 M urea or high pH and studies determining fluorescent polarization values by scanning up and down through a series of temperatures ranging from 15 to 49°C indicates that the translocated proteins are integral. Protein translocation may represent an adaptive response to an altered environment enabling the cell to respond to stress by stabilizing its outer membrane. (Supported by NIH Grant # CA24872)

T-AM-D6

KINETICS OF ALBUMIN-FATTY ACID-MEMBRANE INTERACTION AND TRANSMEMBRANE FATTY ACID TRANSLOCATION. J.B. Bassingthwaighte, S. Little, G. van der Vusse and L. Noodleman, Bioengineering, University of Washington, Seattle, 98195.

Passive diffusional transport of unbound fatty acid across the capillary wall occurs at a rate 1000 times too low to account for observed fluxes in normal hearts, because the concentration of unbound fatty acid is too low, 99.95% of it being bound to plasma albumin. Albumin cannot rapidly traverse the interendothelial clefts to enter the interstitium, therefore plasma-to-myocyte transfer requires consideration of 3 membranes: luminal and abluminal endothelial surfaces and the sarcolemma. Our experimental evidence is that albumin competes with ^{14}C-palmitate- albumin complex for access to the luminal endothelial surface, implying that the same may occur on the other surfaces, as it does on the hepatocyte. Intracellular dissolution and diffusion of fatty acid is facilitated by fatty acid binding protein, FABP (synonymous with Z-protein). Models for fatty acid transport include surface receptors for both albumin and FABP. In one model the 2 types of receptors are considered independent in number and location, implying that free fatty acid translocates by passive vertical and lateral diffusion within the membrane after release from albumin or Z-protein. In another model, a single integral protein acts as a receptor for albumin externally and for FABP internally; these 2 sites may act cooperatively or anticooperatively, the latter having the possible advantage of driving away the transport protein after it delivers its fatty acid substrate to the membrane translocator. Experimental work is needed to distinguish between these models. (Supported by NIH grants HL19139 and RR1243)

T-AM-D7 RECONSTITUTION OF SARCOPLASMIC RETICULUM Ca-ATPASE IN SINGLE SPECIES OF HETEROACID PHOSPHATIDYLCHOLINES WITH DIFFERENT DEGREES OF UNSATURATION.
P.L.J. Matthews, V.S. Ananthanarayanan and K.M.W. Keough, Department of Biochemistry, Memorial University of Newfoundland, St. John's, Newfoundland, Canada A1B 3X9

Ca-ATPase from rabbit SR was purified and reconstituted in one of three heteroacid PC, 16:0-18:0 PC, 16:0-18:1 PC or 16:0-18:2 PC. Endogenous lipids constituted than <0.5% of the total lipid, and residual detergent was < 0.1% of the total lipid. The lipid to protein ratio was 2600-2800:1. The EGTA-inhibitable hydrolysis of ATP in the presence of Ca^{2+} was measured as a function of temperature. This hydrolysis could be uncoupled with A23187. The Arrhenius plot for the enzyme in 16:0-18:0 PC had a discontinuity in the region of the lipid transition temperature. No discontinuities were seen in the other systems (Tc were below 0°C). At 51°C, where all lipids were in the liquid crystalline state, activities were within a factor of two of one another but they increased with increasing unsaturation. The magnitudes of the apparent activation energies in the liquid crystalline state were similar for 16:0-18:0 PC and 16:0-18:1 PC, both being 2-3 times greater than the values for 16:0-18:2 PC. The circular dichroism spectra of the reconstituted systems displayed broad negative elipticities with minima around 223 nm and weak shoulders near 208 nm. The absolute values of elipticities decreased with temperature. Intrinsic typtophan emission spectra at room temperature were of similar magnitude but the maximum intensity in 16:0-18:0 PC was slightly less than that for the other systems. The data suggest that 16:0-18:2 PC might provide a more hospitable environment for the enzyme than do the other lipids, even when all are in the liquid crystalline state. (Supported by the Medical Research Council of Canada).

T-AM-D8 RECONSTITUTION OF N-ETHYLMALEIMIDE-SENSITIVE PROTON PUMP FROM LYSOSOMES. M. Patricia D'Souza*, Suresh V. Ambudkar, J. Thomas August* and Peter C. Maloney. Departments of *Pharmacology and Physiology, Johns Hopkins University School of Medicine, Baltimore, MD 21205.

Lysosomes made by differential and density gradient centrifugation from mice liver injected with Triton WR-1339 were subjected to hypotonic lysis. The membrane vesicles derived from this procedure showed ATP-dependent acidification as judged by the quenching of acridine orange fluorescence. This acidification was not inhibited by oligomycin, ouabain or vanadate, but it was blocked by N-ethylmaleimide, indicating the operation of a proton pump resembling those found in other intracellular granules or vacuoles. To reconstitute this proton pump, lysosomal membranes were solubilized with 1.1% octylglucoside in the presence of 0.4% acetone/ether washed <u>Escherichia coli</u> phospholipid and 20% glycerol. The detergent extract was then mixed with sonicated <u>E</u>. <u>coli</u> phospholipid and additional detergent (to 1.2%) before formation of proteoliposomes by dilution in 150 mM K_2SO_4, 50 mM MOPS/K (pH 7), 0.5 mM EDTA. To test for reconstitution of the proton pump, proteoliposomes were suspended at 3 ug protein/ml in 250 mM sucrose containing 20 mM MOPS/K (pH 7), with 5 uM acridine orange. ATP (2 mM) did not quench fluorescence until valinomcyin (1 uM) was also present; valinomcyin alone gave no response. Further work showed that acidification was indifferent to oligomycin and vanadate, but sensitive to low levels of N-ethylmaleimide (50% inhibition at 10 uM); fluorescence quenching was rapidly reversed by 0.1 uM nigericin or 3 uM carbonylcyanide-p-trifluoromethoxyphenylhydrazone. Such results suggest that lysosomes contain an N-ethylmaleimide-sensitive ATPase which mediates electrogenic proton transport without a direct molecular coupling to other cations or anions.

T-AM-D9 COOPERATIVITY AND CLASSIFICATION OF PHASE TRANSITIONS. APLLICATION TO ONE- AND TWO-COMPONENT PHOSPHOLIPID MEMBRANES. Istvan P. Sugar, Department of Biochemistry, University of Virginia Charlottesville. Virginia 22908 and Institute of Biophysics, Semmelweis Medical University. 1444 Budapest. Hungary (Sponsored by William R. Pearson).

The concept of cooperative unit size of phase transitions is generalized for any system, if the smallest independent subsystem is considered to be the cooperative unit. In order to determine the cooperative unit size in two-component systems new lever rules are derived which contain only directly measurable quantities. The temperature dependence of the cooperative unit size is determined for one- and two-component phospholipid bilayer membranes. Phase transitions are classified on the basis of the cooperativity: a) the transition is cooperative if the cooperative unit size (C.U.) is infinite during the transition. b) partially cooperative if the C.U. changes sharply from infinite to finite value or vica versa during the transition. c) non-cooperative if C.U remains finite during the transition. Since each of these transitions can be first- or second kind, this classification differentiates six classes altogether.

T-AM-D10 FACTORS GOVERNING LIPOSOME UPTAKE BY BONE MARROW MACROPHAGES. T.M. Allen, D. Lee and A. Chonn, Department of Pharmacology, University of Alberta, Edmonton, Alberta, Canada T6G 2H7.

We have examined the uptake of ^{14}C-DPPC-labelled 0.1μ extruded liposomes by cultured murine bone marrow macrophages. Liposome uptake (μmol lipid/mg cell protein) increased linearly with time over a 4 hr time period at 37°C. Non-specific uptake at 4°C averaged approximately 20% of total uptake. For 4 hr incubations uptake was linear up to a liposome concentration of .06 mM and plateaued at higher liposome concentrations at a level of 35 μmol/mg for phosphatidylcholine:phosphatidylserine:cholesterol (PC:PS:CH) liposomes. Inclusion of cholesterol in PC liposomes decreased uptake by 40%-60% while inclusion of sphingomyelin (SM) in PC liposomes decreased macrophage uptake of liposomes in a concentration-dependent fashion with uptake of SM:PC, 4:1 liposomes depressed 80% from that of PC alone. The increased uptake of cholesterol or sphingomyelin-containing liposomes may be a result of the bilayer-tightening properties of these lipids constituents. Inclusion of ganglioside GM_1 in PC liposomes also reduced liposome uptake in a concentration-dependent fashion which plateaued at 10 mol% GM_1. The depression of uptake by GM_1 was not due to surface carbohydrate as inclusion of asialogangliosides in PC liposomes stimulated liposome uptake, as did inclusion of ganglioside $GD1_a$. Nor was the depression due solely to surface negative charge as PS greatly increased uptake while sulfatides in the liposome bilayer depressed uptake of liposomes. The presence of both SM and GM_1 in liposome bilayers resulted in a 10-fold reduction of uptake by macrophages. These observations correlate well with our observations on uptake of liposomes in vivo by liver and spleen.

T-AM-D11 CINEMATIC STUDY OF EFFECTS OF pH ON FORMATION OF MYELIN FIGURES FROM LIPOLYTIC PRODUCTS
Robert O. Scow and Byungkook Lee, NIDDK AND DCRT, NIH, Bethesda, MD 20892
This motion picture film, photographed through a phase contrast microscope at 400 X magnification, shows that long chain fatty acids form myelin figures under certain conditions. Droplets of trioleoylglycerol, suspended from the glass cover slip of a flow-through chamber, were perifused with a solution of pancreatic lipase at pH 6.5. Although 20% of the trioleoylglycerol is hydrolyzed to oleic acid:monooleoylglycerol (9:1) in 30 min at pH 6.5, the oil droplets did not change in appearance until pH of the perifusing fluid was increased to 8.1. Immediately thereafter, the smaller droplets transformed to grey discs while the larger droplets projected myelin figures that continuously grew and changed in shape. Development of the myelin figures probably resulted from entry of partially ionized fatty acids into lipid-water interfaces. Some of the myelin figures developed as thin-walled tubules, which transformed to strings of vesicles and later changed back to tubules. Transformation of tubules to vesicles 8 μm in diam would occur if the outer leaflet of the bilayer acquired 0.1% more fatty acids than the inner leaflet, and the reverse would occur if the difference was reduced. Sodium taurodeoxycholate (17 mM) at pH 8.1 caused rapid dissolution of these myelin figures. When pH of the perifusing fluid was lowered to 5.5, the myelin figures rapidly transformed to oil droplets. Rapid retraction of myelin figures towards sites of lipolysis probably resulted from transfer of protonated fatty acids from leaflets of bilayers to oil lenses located between the leaflets. Return of fatty acids to sites of lipolysis demonstrates that bilayers of the myelin figures were continuous with the monolayers that surrounded the trioleoylglycerol droplets.

T-AM-E1   THERMODYNAMICS OF MINOR GROOVE BINDERS: DISTAMYCIN A AND ITS HOMOLOGUES. Luis A. Marky, Denise Zaunczkowski, Robert Ferrante, and Kenneth J. Breslauer. Department of Chemistry, Rutgers University, New Brunswick, NJ 08903.

Distamycin A (which corresponds to the n=3 drug shown below), is a monocationic, basic oligopeptide which exhibits antibacterial, antifungal, and antiviral activities. The drug binds to the minor groove of B-DNA in a non-intercalative manner. The drug-DNA complex is stabilized by contributions from peptide-nucleotide hydrogen bonding, hydrophobic forces, and electrostatic interactions. We have shown that distamycin A exhibits a very high binding affinity for the poly dAT·poly dAT duplex ($K \sim 10^8$). We also have shown that the strong binding event is overwhelmingly enthalpy driven ($\Delta H_b = -18.5$ kcal/mol). These results previously have been reported. The work reported here, which is an extension of these previous studies, is designed to evaluate the influence and thermodynamic contribution of the pyrrole rings on DNA binding. To this end, we have studied the DNA binding of two distamycin A homologues in which n=4 and n=5 as shown below.
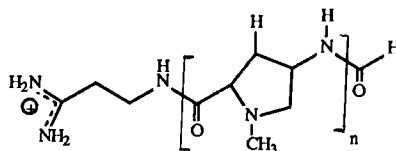
Distamycin A homologues   n = 3, 4, and 5

Specifically, we have used a combination of spectroscopic and calorimetric techniques to measure the thermodynamics for association of distamycin A and its homologues with the poly dAT·poly dAT duplex at low ionic strength. Our results reveal the following significant observations: 1) Drug binding increases the thermal stability of the host duplex. The magnitude of this ΔT_m depends on the number of pyrrole groups in the drug. Significantly, however, each additional pyrrole group between 3 and 5 induces a smaller incremental increase in the melting temperature of the host duplex. 2) These drug-induced thermal stabilizations correspond to binding constants of $\sim 10^8$ for distamycin A (n=3) and its two homologues (n=4 and n=5). 3) The binding enthalpies of the n=4 and n=5 homologues are much less exothermic than the corresponding binding enthalpy of distamycin A. The thermodynamic driving force for the binding of these latter two homologues is significantly less enthalpically driven than the binding of distamycin A. This work is supported by NIH grant GM-34469.

T-AM-E2 ^{1}H NMR STUDIES ON THE INTERACTION BETWEEN DAUNOMYCIN AND THE OLIGOMERIC DUPLEX d(CGTACG)$_2$ David P. Remeta, Bruno Van Hemelryck, Barbara L. Gaffney, Roger A. Jones, and Kenneth J. Breslauer, Department of Chemistry, Rutgers University, New Brunswick, NJ 08903

High-resolution NMR studies on ligand-DNA interactions has greatly facilitated elucidation of the solution structure of drug-DNA complexes. Employing a combination of one- and two-dimensional proton NMR techniques, we have characterized the structural features of the complex formed between daunomycin (an anthracycline antitumor drug) and the oligomeric duplex d(CGTACG)$_2$. Applying phase sensitive 2D correlation (COSY) and 2D nuclear Overhauser effect (NOESY) spectroscopic methods, we initially assigned the proton resonances of the hexamer in the absence of drug. Our results are consistent with previous assignments based on 1D NOE measurements (A.M. Gronenborn et al., Biochem. J. 221,723 [1984]). Addition of daunomycin to d(CGTACG)$_2$ in increasing drug:DNA ratios destroys the conformational symmetry of the hexamer and results in the appearance of numerous drug-bound duplex resonances throughout the ^{1}H spectrum. Significantly, at a ratio of one daunomycin molecule per hexamer, several of the drug-free duplex signals are observed to be in slow exchange with (and hence related to) three drug-bound duplex resonances. Titration of the hexamer with additional drug reveals that the three drug-bound duplex resonances correspond to two 1:1 and one 2:1 drug:hexamer complexes in equilibrium with the drug-free duplex. Magnetization transfer and inversion recovery experiments coupled with NOESY and double quantum filtered COSY techniques permitted direct assignment of the drug-bound duplex resonances in the base and imino proton regions of the spectrum. Based on our NMR data, we propose a solution structure for the daunomycin:d(CGTACG)$_2$ complex. This proposed structure will be compared with that of the solid-state structure gleaned from x-ray studies (Quigley et al., Proc. Natl. Acad. Sci. USA, 77,7204 [1980]). Supported by NIH GM-34469.

T-AM-E3   A STOPPED-FLOW H-D EXCHANGE KINETICS STUDY OF SPERMINE-POLYNUCLEOTIDE INTERACTION. H.S. Basu[1], R.H. Shafer[2], L.J. Marton[1,3], [1]Brain Tumor Research Center of the Department of Neurological Surgery, School of Medicine, [2]the Department of Pharmaceutical Chemistry, School of Pharmacy, [3]Department of Laboratory Medicine, University of California, San Francisco, CA 94143.

The rates of H-D exchange for imino and amino protons in adenosine, calf-thymus DNA, poly(dA-dT), poly(dG-dC) and poly(dG-me^{5}dC) were determined using stopped-flow kinetic methods in the presence of various concentrations of Tris, imidazole, Mg^{2+}, and spermine in citrate buffer (pH7, 25°C). CD studies showed that all the polynucleotides always remain in B-form under these conditions. An increase in concentration of Tris and imidazole from 5 μM to 20 mM caused an increase in the rates of exchange of both fast exchanging imino and slow exchanging amino protons. The limiting rates of exchange at infinite concentration of catalysts were found to be different for fast and slow exchanging protons. These results indicate that imino and amino protons of B-DNA exchange asymmetrically from two different open states. An increase in the concentration of spermine decreased the rate of exchange of imino protons of calf thymus DNA, poly(dG-dC), and poly(dG-me^{5}dC) but increased the rate of exchange of the imino protons of poly(dA-dT) without affecting the exchange rate of the amino protons of any of the polynucleotides. These results are interpreted in terms of possible spermine induced bending of oligonucleotides of specific sequence suggested by theoretical model building studies. Supported by NIH Grants CA 13525 and CA 27343 and NCDDG Grant 37606.

T-AM-E4   HEXAMMINERUTHENIUM (III) CHLORIDE - A HIGHLY EFFICIENT PROMOTER OF THE B-DNA TO Z-DNA TRANSITION.   T.J. Thomas and Ronald P. Messner, Department of Medicine, University of Minnesota, Minneapolis, MN 55455.

Synthetic polynucleotides containing the alternating purine-pyrimidine sequences are known to undergo a facile transition from the right-handed B to the left-handed Z conformation in the presence of salts, polyamines and inorganic complexes. Among the various agents reported to provoke this transition, $Co(NH_3)_6^{3+}$ is the most efficient trivalent cation reported in the literature. We studied the effect of $Ru(NH_3)_6^{3+}$ on the conformation of poly(dG-m^{5}dC)·poly(dG-m^{5}dC) using circular dichroism spectroscopy. In the presence of 50 mM NaCl, the midpoint concentration of $Ru(NH_3)_6^{3+}$ to induce the B to Z transition of this polymer is 4 uM, which may be compared to that of $Co(NH_3)_6^{3+}$ at 5 uM. A straight line is obtained on plotting $\ln[Na^+]$ vs. $\ln[Ru(NH_3)_6^{3+}]$. We have further calculated the kinetics of B to Z transition induced by $Ru(NH_3)_6^{3+}$ and found that this cation is among the most efficient promoters of this transition in synthetic DNAs. The effects of $Ru(NH_3)_6^{3+}$ and other ruthenium compounds on the conformation of poly(dG-dC)·poly(dG-dC), poly(dA-dC)·poly(dG-dT) and poly(dA-dT)·poly(dA-dT) have also been studied. Calf thymus DNA is used as a control.

The induction and stabilization of Z-DNA by $Ru(NH_3)_6^{3+}$ are of particular interest since ruthenium compounds are potential cancer chemotherapeutic agents. A model for the stabilization of Z-DNA by $Ru(NH_3)_6^{3+}$ is proposed.

T-AM-E5   NUCLEIC ACID DUMBELLS *Dorothy Erie,Wilma Olson, Roger Jones, Navin Sinha, and Kenneth Breslauer, Departments of Chemistry and Microbiology, Rutgers University, Piscataway, NJ 08854*

We have designed and synthesized the 24-mer sequence d(TTCCTTTTGGAATTCCTTTTGGAA). We had three reasons for choosing this sequence. 1) It possesses 5' and 3' domains that can loop back on themselves to form a dumbell-shaped double hairpin structure, as shown below. 2) The 5' end can be phosphorylated enzymatically to produce a "gapped dumbell" with a 5' phosphate in the interior of the helix. 3) The core duplex, d(GGAATTCC)$_2$, has been characterized, thereby providing a well-defined reference state.

We used gel electrophoresis under non-denaturing conditions to characterize the size of the native structures for both the unphosphorylated and phosphorylated sequences. These results reveal that the native forms of both 24-mer sequences travel similarly to a 12 base pair sequence. We also employed calorimetric and spectroscopic techniques to characterize thermodynamically their solution structures. The resulting data (which are presented in the table) provide strong circumstantial evidence for formation of the dumbell-shaped double hairpin structures shown below. The significant results are: 1) The structure formed by the 24-mer sequence melts with a transition enthalpy equal to that of the core duplex. Thus the gap in the core duplex of the dumbell does not affect its transition enthalpy. 2) Incoporation of a 5' phosphate group into

Structure	ΔH* (kcal/mol)	ΔS* (e.u.)	∂Tm ∂log[Na+]	Δl /phosphate	f(conc)
GGAATTCC CCTTAAGG	58		12.3	0.096	yes
GGAATTCC CCTTAAGG (loop)	55	173	11.1	0.058	no
GGAATTCC CCTT̂AAGG (loop) (kinased)	45	143	13.8	0.058	no

the gap results in thermal destabilization of the dumbell-shaped structure. The salt dependence of this destabilization reveals its electrostatic origin. 3) The phosphorylated gapped dumbell resists ligation. 4) The thymine residues in the hairpin loops behave thermodynamically as denatured "coils". These results will be interpreted in terms of potential structural models. The effect of directionality and loop size also will be discussed.

T-AM-E6   ELECTROSTATIC FORCES IN NUCLEIC ACID STRUCTURE   by George R. Pack, C. V. Prasad and Linda Wong,   University of Illinois College of Medicine at Rockford, 1601 Parkview Ave., Rockford, Illinois 61107

The distribution of electrolyte charge surrounding various DNA fragments has been calculated using both Poisson-Boltzmann and Monte Carlo techniques. Models of different conformations of DNA, using atomic coordinates taken from x-ray diffraction data and atomic charges from molecular orbital calculations, have allowed estimates of the electrolyte charge in the grooves and at different loci around the nucleic acid surface. This, in turn, provides a basis for the calculation of the forces that the electrolyte environment exerts on the atoms of the DNA. All of the calculations to be presented have assumed that the water could be represented as a dielectric continuum. Calculations of the free energy of the DNA-environment system have been done for various conformations of isolated DNA helices as well as for hexagonal arrays of helices at several inter-helical distances. Comparison with experiment allows an assessment of the degree to which the aqueous environment may be regarded as a continuum.

T-AM-E7   SPECTROSCOPIC AND COMPUTATIONAL PROBES OF VALENCE ELECTRONS IN DNA COMPONENTS.

Shigeyuki Urano, Zinaida Slutskaya and Pierre R. LeBreton, Department of Chemistry, University of Illinois at Chicago, Chicago, Illinois 60680.

Photodetachment spectroscopy and ab initio molecular orbital calculations with STO-3G, STO-3G* and 4-31G basis sets have been employed to characterize valence orbital structure in nucleotide bases, nucleosides, ribose model compounds and phosphate esters. After scaling to the spectroscopic data the calculations have provided binding energies and electron distributions of the occupied orbitals of 2'-deoxycytidine 5'-phosphate in the neutral state, and in the anionic state, both in the presence and in the absence of positive counter ions. The results provide insight concerning the influence of valence orbital structure on nucleotide stacking interactions and on DNA alkylation patterns.

T-AM-E8   TOPOLOGICAL EFFECTS ON THE GEL ELECTROPHORESIS OF DNA. Stephen D. Levene and Bruno H. Zimm; Department of Chemistry, University of California, San Diego, La Jolla, CA 92093.

The effect of high electric fields ($\geq$ 5 v/cm) on the gel electrophoretic mobility of open circular DNA in agarose differs dramatically from that on linear molecules of the same molecular weight. At high fields, sufficiently large circular forms are prevented from migrating into the gel while linear molecules and smaller circular DNAs migrate normally. This effect is strongly field dependent, affecting circular molecules of decreasing size with increasing field strength.

We have studied this effect with a series of plasmid DNAs ranging from 3.3kbp to 56kbp in size using continuous and reversing-pulse electric fields. Application of reversing-pulse fields abolishes the effect under certain conditions and supports a model for the gel electrophoresis of circular DNA where circular forms are trapped by engaging the free end of an agarose gel fiber.

T-AM-E9   DYNAMICS OF DNA DURING ELECTRIC FIELD INVERSION GEL ELECTROPHORESIS. G. Holzwarth, Chad McKee, and Susan Steiger, Department of Physics, Wake Forest University, Winston-Salem, NC 27109.

The dynamic response of DNA in agarose gels to electric fields which alternate direction cyclically every 1 to 30 sec is being explored by us using fluorescence-detected linear dichroism (FDLD) of ethidium-bromide stained DNA. Unlike traditional steady fields, cyclically alternating fields can separate DNAs with M as large as 1000 kbp, for example, the DNAs of individual chromosomes of yeast. We are trying to understand the molecular mechanism of this separation.

We first use field inversion gel electrophoresis to separate a DNA sample such as yeast or a lambda ladder into bands of unique, known M. We then shine a laser beam through a particular band in the gel and use FDLD to measure the orientation, relaxation, and "resonance" responses of these DNA coils to the cyclically alternating electrophoretic field. Preliminary FDLD measurements show that 1) the DNA is highly oriented even at very low fields; 2) the extent of orientation is highly non-linear in the electric field intensity; 3) the orientation shows overshoots at particular values of the field; 4) orientation time decreases with increasing field but increases markedly with M; 5) the relaxation rates for disorientation differ from those for orientation and are not a single exponential. During field inversion, the DNA molecules pass rapidly from an oriented state, through a disoriented state, and then back to an oriented state. These results will be compared to existing molecular theory. (Support by the North Carolina Biotechnology Center and the NSF is gratefully acknowledged).

T-AM-E10 UNIDIRECTIONAL PULSED FIELD ELECTROPHORESIS OF SINGLE AND DOUBLE STRANDED DNA IN AGAROSE GELS: ANALYTICAL EXPRESSIONS RELATING MOBILITY AND MOLECULAR LENGTH AND THEIR APPLICATION IN THE MEASUREMENT OF STRAND BREAKS[1]
John Clark Sutherland, Denise C. Monteleone, JoAnn H. Mugavero and John Trunk
Biology Department, Brookhaven National Laboratory, Upton, NY 11973

Unidirectional pulsed field electrophoresis improves the separation of single stranded DNA molecules longer than 20 kilobases (kb) in alkaline agarose gels compared to static field electrophoresis. The greatest improvement in separation is for molecules longer than 100 kb. The improved resolution of long molecules with pulsed field electrophoresis makes possible the measurement of lower frequencies of single strand breaks. The analytical function that relates the length and mobility of single stranded DNA electrophoresed with a static field also applies to pulsed field separations. Thus, the computer programs used to measure single strand breaks are applicable to both pulsed and static field separations. Pulsed field electrophoresis also improves the dispersion of double stranded DNA in neutral agarose gels. The dispersion function for double stranded DNA separated by pulsed field electrophoresis is a superset of the function for single stranded DNA. The coefficients of this function can be determined by iterative procedures.

T-AM-E11 ANALYSIS OF CELL GENOMIC DNA BY TWO-DIMENSIONAL AGAROSE GEL ELECTROPHORESIS. Saibal K. Poddar and Jack Maniloff. Departments of Microbiology and Immunology, University of Rochester, Medical Center Box 672, Rochester, NY 14642.
A two-dimensional fingerprinting technique has been developed that allows large, cell genome-size DNA's to be analyzed by restriction endonuclease cleavage and separation of DNA fragments by agarose gel electrophoresis. In this method, chromosomal DNA is digested with a restriction endonuclease and the fragments are analyzed by agarose gel electrophoresis. The entire first dimension DNA fragment distribution is then transferred from the gel to a DEAE cellulose membrane and digested by a second restriction endonuclease. The transfer facilitates the second digestion; since all DNA fragments are uniformly exposed to high specific activity nuclease, and agarose contaminants are absent so all nucleases can be used. The geometry of the DNA on the membrane surface also improves final gel resolution. The fragment distribution on the DEAE cellulose membrane is separated by a second agarose gel electrophoresis, with the electric field perpendicular to the original electrophoresis direction. This generates a two-dimensional fingerprint of the chromosome. Equations have been derived to determine the genome size and number of cleavage sites from an analysis of the distribution of fragment lengths. Genome sizes of Escherichia coli strain JM101 and two strains of the mycoplasma Acholeplasma laidlawii have been measured by this method are in agreement with published values. Other uses of two-dimensional fingerprinting for studies of prokaryotic and eukaryotic genome structure and organization will be described.

T-AM-F1   STRUCTURAL AND IMMUNOCYTOCHEMICAL STUDIES OF BEHAVIORALLY-RESPONSIVE PERMEABILIZED
PARAMECIUM. S J. Lieberman, J R. Dedman[+], T. Hamasaki & P. Satir, Dept. of Anatomy &
Structural Biology, Albert Einstein Coll. of Med., Bx., NY & [+]Univ. Texas Med. Sch., Houston, TX.
   We have utilized a well-defined permeabilized cell system for studying structural and
immunocytochemical features of the mechanism of Ca^{2+} control of ciliary reversal. Forward
swimming, living paramecia, when quick-fixed for SEM, show metachronal waves and an effective
stroke toward the posterior. Upon treatment with Triton X-100, swimming ceases and cilia project
perpendicularly from the cell surface. Thin sections of these cells indicate that the ciliary,
cell, and alveolar membranes are greatly disrupted or missing and that the cytoplasm is also
extracted. The permeabilized paramecia can be reactivated. Motion analysis of cells reactivated
with Mg^{2+} and ATP in low Ca^{2+} buffer (pCa 7) shows that 81% swim forward at speeds averaging $167\pm$
25 µm/sec. When these cells are quick-fixed, the metachronal wave patterns of living, forward
swimming cells reappear. Permeabilized cells reactivated in high Ca^{2+} buffers (pCa 5) swim
backwards and SEM reveals a metachronal wave pattern with an effective stroke toward the anterior.
The behavioral responses of these premeabilized cells depend on interaction with molecules that
remain bound to the ciliary axonemes throughout the extraction and reactivation procedures.
Immunofluorescent and immunogold studies with both preembedding and postembedding labeling methods
have shown that calmodulin (CaM) is one such molecule that could serve as the Ca^{2+} sensor of the
axoneme. Localization of tubulin on axonemal doublets and on central pair microtubules serves as
a control. CaM is localized within the demembranated axonemes. Preliminary results suggest that
the localization does not correspond to the positions of the dynein arms.
Supported by grants from USPHS

T-AM-F2   A NEW METHOD OF REACTIVATION OF OUTER DYNEIN ARM DEPLEATED SPERM TAIL AXONEMES .
W.S. Sale and L.A. Fox, Dept. of Anatomy-Cell Biology, Emory University School of
Medicine, Atlanta, Georgia 30322.
   We have developed a means of efficient extraction of the dynein 1 outer arms from demembranated
sea urchin sperm tails. 20 µL of fresh, undiluted L. pictus spermatozoa were suspended in 0.5ml
high salt demembranation buffer (HS cells) containing 0.6M KCl,10mM Tris-base,pH 8.15,2mM EGTA,
50 µM cAMP,1mM dithiothreitol,0.05% w/v Triton-x-100. Control cell (C cells) demembranation
buffer contained 0.15M KCl. After 3 min. 20 µL of demembranated cells were transfered to 2.5mls
reactivation buffer (ATP varied as needed,10mM Tris-base,pH 8.15,2mM $MgSO_4$,1mM dtt,0.25M potassium
acetate). Electrophoresis and E.M. of HS cells revealed complete extraction of dynein 1 proteins
and outer dynein arms. All other axonemal heavy chains and structures (eg. inner arms, spokes,
central pair, etc.) remained intact. (C cells had 100% intact dyneins based on electrophoresis
and E.M.) HS cells have 1/2 the beat frequency of C cells for any given [MgATP] over a range of
2.5 µM-0.5mM. Beat frequency for both HS cells and C cells closely fit Michaelis kinetics with
calculated Km's of 0.056mM and 0.13mM ATP, respectively. Waveforms for both HS + C cells were
fairly symmetrical at [ATP] < 0.1mM. Important factors for reactivation of HS cells included:
time in demembranation buffer; use of KCl for extraction; high EGTA and no added Ca^{++} in
demembranation buffer; and relatively low [ATP] and not less that 0.25M K^+ acetate in the reac-
tivation buffer. HS cells could be induced to form stationary principal bends in Ca^{++} and 1mM
ATP as reported before for C cells. Direct measurements of elastase induced sliding disruption,
in 1 mM ATP, revealed that HS cell microtubules slide at 7µm/sec. Under the same conditions C
cell microtubules slide at 14 µm/sec. As described previously, these results show that inner arms
generate 1/2 beat frequency and 1/2 sliding rates compared to intact axonemes. These methods and
results offer a new and generally available opportunity to study functional reconstitution of
outer dynein arm components, to determine the composition and molecular structure of the inner row
of dynein arms, and to investigate the components which effect Ca^{++}-induced stoppage and cAMP –
induced activation of the axoneme.

T-AM-F3   SPECIFIC INTERACTION OF VINCULIN WITH α-ACTININ MEASURED WITH FLUORESCENCE ENERGY
TRANSFER. Daniel H. Wachsstock, James A. Wilkins, and Shin Lin, Dept. of Biophysics, Johns Hopkins
University, Baltimore, MD. 21218
   Vinculin and α-actinin are cytoskeletal proteins present at focal contacts of the ventral sur-
face of cultured fibroblasts where the cell is in close contact with the underlying substrate. We
labelled α-actinin with fluorescein-5-isothiocyanate (FITC) and vinculin with 5-(iodoacetamidoethyl)
-aminonaphthalene-1-sulfonic acid (IAENS). A mixture of 0.1 mg/ml IAENS-vinculin (donor, 1.8-2.0
mol IAENS/mol) and 0.2 mg/ml FITC-α-actinin (acceptor, 0.8-1.0 mol FITC/mol) in 20 mM NaCl/1 mM β-
mercaptoethanol/0.005% NaN_3/20 mM Tris (pH 7.5) showed a 28% quench, compared to labelled vinculin
alone. The quench was due to energy transfer and not re-absorption, as indicated by the decrease
in fluorescence lifetime (measured by time-resolved fluorometry) of the IAENS equalling the degree
of quench. Quench of IAENS-vinculin was dependent on the concentration of FITC-α-actinin;
Scatchard analysis gives a dissociation constant in the µM range. Quench was inhibited by excess
unlabelled α-actinin, and by reaction of the acceptor protein with p-chloromercuribenzoate. Vary-
ing the concentrations of salt, Ca^{2+} and Mg^{2+} produced no major effect. The interaction was also
studied by equilibrium gel filtration. We found that IAENS-vinculin (50 µl of 0.1 mg/ml) had a
slightly greater elution volume when the Sephacryl S-300 column was equilibrated with unlabelled
α-actinin (0.8 mg/ml), indicating a higher effective Stokes radius due to the interaction of the
two proteins. This study supports the conjecture that vinculin and α-actinin may be links in a
chain that connects cytoskeletal actin filaments to the cell membrane. Supported by NIH grant
GM-22289.

T-AM-F4   A CALCULATION OF THE GTP CAP SIZE BASED ON OBSERVED FREQUENCIES OF MICROTUBULE CATAS-TROPHE. W.A. Voter, E.T. O'Brien and H.P. Erickson, Anatomy Dept., Duke U., Durham, NC 27710

In the generally accepted GTP-tubulin cap model explaining dynamic instability (a) addition of GTP subunits occurs at a constant rate onto polymers with a GTP cap; (b) GTP hydrolysis occurs as a first order reaction subsequent to incorporation of GTP subunits; (c) polymers whose GTP cap size goes to zero stop growing and depolymerize (catastrophe). In our treatment, we iterate over small time intervals (Δt) treating GTP hydrolysis and subunit addition as stochastic processes. For given values of the hydrolysis rate (k_h) and growth, the computer calculation quickly relaxes to a fixed distribution of cap sizes, i.e. we determine a distribution $P(n)$ where P is the probability that a polymer will have n GTP subunits (cap size n). The goal of our modeling was to determine parameters for which $P(0)$, the probability of achieving cap size zero during Δt, would approximate the observed frequency of disassembly. Recently, values for the duration of the growth phase (2.9 min) and the growth rate (0.63 um/min) were observed for in vitro assembly of tubulin (Nature 321: 605). For a growth rate of 17.1 subunits/sec, we varied k_h to obtain the value of $P(0)$ closest to 1/2975 for $\Delta t = 1/17.1$ sec. The best fit was obtained for $k_h = 2.14$ s^{-1} yielding an average cap size of 8 subunits. The value of $P(0)$ was found to be strongly dependent on growth rate. If the growth rate was doubled, $P(0)$ was reduced by a factor of 690, meaning negligible loss of caps and a doubling of the average cap length. If growth was halved, $P(0)$ increased by a factor of 8.7, giving a great increase in cap loss and catastrophic disassembly and a halving of the average cap length. An important finding of this approach is that the predicted average cap size is much smaller and k_h is much larger than in previous treatments.

T-AM-F5   THEORETICAL ANALYSES OF THE ELASTICITY OF CYTOSKELETAL NETWORKS. R. Nossal. Physical Sciences Lab., DCRT, NIH, Bethesda, Maryland 20892.

Several models relating to the gelation and elasticity of complex cytoskeletal networks are formulated and investigated. Kinetic equations for reversible elongation of nucleated actin filaments are analyzed when the filaments are acted upon by capping proteins and crosslinking factors. The low frequency elastic shear modulus of a network, G, is derived by using theory developed by Pearson and Graessley (Macromolecules 11, 528 (1978)). Analytical expressions are obtained that relate G to chain growth kinetics, the number of nucleation sites, and the amount of capping and crosslinking protein. Elasticity curves which relate G to such factors as the association constant for crosslinking and the amount of crosslinking protein are determined. These curves then are used to ascertain solation-gelation phase contours. The manner in which actin bundling factors affect the elastic modulus also is investigated.

T-AM-F6   THE USE OF ELECTROPORATION (EP) TO INSERT ANTIBODIES TO MYOSIN LIGHT CHAIN KINASE (MK-Ab) INTO RAT ALVEOLAR MACROPHAGES (AM). A.K. Wilson, W.D. Claypool and P. de Lanerolle, Depts. of Physiology and Biophysics, and Medicine, Univ. of Illinois at Chicago, Chicago, Il. 60612.

We have used EP to introduce antibodies into AM to study the mechanisms that regulate cell motility. EP involves voltage discharge from a bank of capacitors (effective capacitance 14uF) through a chamber containing cells suspended in a solution that includes the protein to be incorporated. This procedure appears to create transient pathways in the plasma membrane that permit the entry of macromolecules into the cells. EP was used to introduce proteins into AM at voltages ranging from 0-1200V at a constant amperage. Viability, as judged by trypan blue exclusion and directed migration of AM in a multiwell chemotaxis chamber, decreased rapidly at voltages greater than 900V. The amount of BSA that was incorporated increased up to 900V. At greater than 900V there was less BSA per cell suggesting damage to the cell membrane and back diffusion of the BSA out of the cells. Microscopic examination indicated that nearly every cell incorporated BSA when AM were shocked with 700V. We have also used EP to evaluate the effect of control or MK-Ab on AM motility. We evaluated the effect of MK-Ab (PNAS 78; 4738, 1981) because phosphorylation of the 20 kD light chain of macrophage myosin by myosin light chain kinase is postulated to be critically involved in AM migration. EP of MK-Ab into AM significantly inhibited directed migration as compared to cells shocked with control antibody. We conclude from these experiments that EP is a highly effective method for introducing biochemical probes into living cells to study in vivo physiological processes.

T-AM-F7   ELECTRICAL MEASUREMENTS OF CELL BEHAVIOR IN TISSUE CULTURE, I. Giaever and C.R. Keese, General Electric Corporate Research and Development, PO Box 8, Schenectady, NY 12301

Mammalian fibroblasts have been cultured on small electrodes and subjected to weak AC fields that have no apparent effects on the cells. By measuring the impedance of the electrode, we can detect changes that are correlated with aspects of cell behavior including attachment, spreading and locomotion. Based on the dependence of the impedance upon the frequency of the applied signal, we have shown that the system allows one to probe, in real time, the narrow space between the ventral surface of a layer of cells and the substrate.

The fluctuations of the impedance values that are associated with cell motion have been extensively analyzed for predominating frequencies of cell origin. No such frequency has been found; however, the power density spectrum of the fluctuations is nearly an order of magnitude higher for a transformed cell line (WI-38 VA13) than for its normal counterpart (WI-38), and the frequency dependence of the power spectrum appears to be steeper for cancer cells.